



NATIONAL TECHNICAL UNIVERSITY OF ATHENS

SCHOOL OF CIVIL ENGINEERING

**DEPARTMENT OF WATER RESOURCES AND
ENVIRONMENTAL ENGINEERING**

DIPLOMA THESIS:

**Development of methodology for the design of Sediment Bypass
Tunnels (SBTs) in dam reservoirs**

KEMERIDIS MARIOS

Supervisor: Andreas Efstratiadis, Assistant Professor, NTUA

Table of Contents:

[ΠΡΟΛΟΓΟΣ](#): Page 3

[ABSTRACT](#): Page 4

[ΠΕΡΙΛΗΨΗ ΣΤΗΝ ΕΛΛΗΝΙΚΗ](#): Page 5

Chapters:

1. [Introduction](#)

1.1. [General Information](#): Pages 6-8

1.2. [Project Outline](#): Page 8

2. [Area of Interest – Ladonas Dam Reservoir](#): Pages 9-10

3. [Rainfall IDF Curve Methodology for Regular Rainfalls](#): Pages 11-13

4. [Determination of Rainfall Limits for Sedimentation](#): Pages 14-15

5. [Calculation of Yearly Sedimentation via R.U.S.L.E.](#)

5.1. [The rainfall erosivity factor, R](#): Pages 16-18

5.2. [The soil erodibility factor, K](#): Pages 19-22

5.3. [The topographic factor, LS](#): Pages 23-24

5.4. [The land coverage factor, C](#): Pages 25-32

5.5. [The erosion control/protection factor, P](#): Page 33

5.6. [Calculation of sediment volume](#): Pages 34-35

6. [Creation of a Tunnel Flow Model](#)

6.1. [Creation of a rainfall event input](#): Pages 36-42

6.2. [Height-volume equation parameters](#): Pages 43-48

6.3. [Constant Parameters of the Tunnel Flow Model](#): Pages 48-52

6.4. [Main Tunnel Flow Model](#): Pages 52-55

6.5. [Additional processes](#): Pages 55-57

7. [Calculation of Tunnel Material Loss due to Sediment Flow](#)

7.1. [Constant Parameters](#): Pages 58-61

7.2. [Calculation of the bed load sediment volume](#): Pages 61-65

7.3. [Calculation of the tunnel abrasion/material loss](#): Pages 65-68

7.4. [Estimation of the annual repair cost of the tunnel](#): Pages 68-70

8. [Conclusions](#)

8.1. [Advantages of the process of this project](#): Page 71

8.2. [Overview of the results for the Ladonas reservoir](#): Pages 71-72

8.3. [Possible future improvements of this project](#): Page 72-73

[References](#): Pages 74-77

ΠΡΟΛΟΓΟΣ

Η διπλωματική εργασία αυτή αποτελεί το τελικό κομμάτι της προπτυχιακής μου πορείας στην Σχολή Πολιτικών Μηχανικών του Εθνικού Μετσοβίου Πολυτεχνείου. Πολλά από τα στοιχεία που συμπεριλαμβάνονται σε αυτή προέρχονται από γνώσεις που έλαβα κατά την διάρκεια των περασμένων πέντε ετών, και ιδιαίτερα από τον Τομέα Υδατικών Πόρων και Περιβάλλοντος.

Αφορμή για το ίδιο το θέμα της εργασίας αυτής αποτελεί η αναφορά της τεχνολογίας των σηράγγων εκτροπής φερτων στο μάθημα «Υδραυλικές Κατασκευές και Φράγματα» από τον διδάσκων του μαθήματος αυτού, κ. Ανδρέα Ευστρατιάδη, Επίκουρο Καθηγητή Ε.Μ.Π., ο οποίος και επέβλεψε την συγκεκριμένη διπλωματική εργασία. Οι παρατηρήσεις του σχετικά με πολλαπλά τμήματα της διαδικασίας που ακολουθήθηκε συνέδραμαν καθοριστικά στην βελτίωση της εργασίας αυτής. Ούτως ή άλλως, η ιδέα την οποία υλοποίησα για τον διαχωρισμό ημερησίων βροχοπτώσεων σε βήματα μέσω της μεθόδου των ομβρίων καμπυλών ήταν κατόπιν δικής του πρότασης. Επίσης, τον ευχαριστώ θερμά γενικότερα για την συνδρομή του κατά την εκπόνηση της διπλωματικής μου εργασίας καθώς και για το γεγονός ότι θεώρησε θετική την σιγήθειά μου να εμφανίζομαι κάθε άλλη εβδομάδα με μια τελείως διαφορετική υπολογιστική διαδικασία από την προηγούμενη.

Τέλος, ευχαριστώ την οικογένειά μου, καθώς και τους φίλους μου, που με υποστήριξαν καθ'όλη την διάρκεια των σπουδών μου.

Κεμερίδης Μάριος

Αθήνα, Νοέμβριος 2024

Abstract

The present project aims towards the development of a procedure for the calculation of, first, the sedimentation at the reservoir of a dam and, second, the annual cost of damages that a sediment bypass tunnel at such a reservoir would incur during its operation under such a rate of sedimentation. The procedure is purposefully made to be based on simplistic input data so that it is usable even when extensive field surveys at a reservoir site have not, or cannot, be conducted. Then, the end results based on that data can inform us on the following: 1) whether the sedimentation rate at the reservoir is high enough to justify the construction of a sediment bypass tunnel and 2) whether a sediment bypass tunnel is a solution financially feasible in regards to its annual maintenance costs. This project aims to showcase the aforementioned procedure based on the real-life example of the Ladonas reservoir in Greece. That said, the process has been made “open” enough to accommodate for the input data of any reservoir, if used correctly.

ΠΕΡΙΛΗΨΗ ΣΤΗΝ ΕΛΛΗΝΙΚΗ

Η παρούσα διπλωματική εργασία στοχεύει στην ανάπτυξη μιας διαδικασίας για τον υπολογισμό, πρώτον, της εισροής φερτών στον ταμιευτήρα ενός φράγματος και, δεύτερον, του ετησίου κόστους των ζημιών που θα προκαλούνταν σε μια σήραγγα εκτροπής φερτών στον ίδιο ταμιευτήρα κατά την λειτουργία της εν' λόγω σήραγγας υπό τον προηγουμένως υπολογισμένο ρυθμό εισροής φερτών. Η διαδικασία έχει σκοπίμως σχεδιαστεί έτσι ώστε να βασίζεται σε απλοϊκά δεδομένα εισόδου και έτσι να μπορεί να χρησιμοποιηθεί ακόμη και όταν δεν έχουν διεξαχθεί, ή δεν μπορούν να διεξαχθούν, εκτεταμένες επιτόπιες έρευνες στην περιοχή ενός ταμιευτήρα. Στην συνέχεια, τα τελικά αποτελέσματα που βασίζονται στα δεδομένα αυτά μπορούν να μας πληροφορήσουν για τα εξής: 1) εάν ο ρυθμός εισροής φερτών στον ταμιευτήρα είναι αρκετά υψηλός ώστε να δικαιολογεί την κατασκευή μιας σήραγγας εκτροπής φερτών και 2) εάν μια σήραγγα εκτροπής φερτών είναι μια λύση οικονομικά εφικτή όσον αφορά το ετήσιο κόστος συντήρησής της. Αυτή η εργασία στοχεύει στο να παρουσιάσει την προαναφερθείσα διαδικασία με βάση το πραγματικό παράδειγμα του ταμιευτήρα Λάδωνα στην Ελλάδα. Παρ' όλα αυτά, η διαδικασία έχει γίνει αρκετά "ανοιχτή" ώστε να δύναται να λειτουργήσει με τα δεδομένα εισόδου οποιουδήποτε ταμιευτήρα, εάν χρησιμοποιηθεί ορθά.

Chapter 1 – Introduction

1.1 General Information

Dams are universally not only a secure and reliable source of water for irrigation and water supply but also for production of electricity at a scale that is not currently attainable through any other renewable energy source. However, the opposition towards the construction of new dams and the plethora of negative reactions towards existing ones, stem from a painfully obvious point: when one blocks the flow of a river with a considerably sizeable construction what should go downstream, does not, in fact, arrive there anymore. And indeed, the more complex problems caused by dams can be summarized into that previous statement. Those are, among others, the forced stabilization of downstream flow, the prevention of movement of migratory river fish, and-more importantly in regards to this project-the sedimentation of the reservoir. The former two issues have their own complexities: the allowed environmental flow must vary depending on the expected monthly rainfall and then fish ladders and elevators as well as other similar solutions are neither easy to plan or build and require designs specific to the situation of each dam. However, both of those problems, whilst undoubtedly crucial, do not endanger the very existence of a dam's reservoir itself; sedimentation does. And with an average worldwide sedimentation rate of 0.96%[\[32\]](#) there is more than good enough reason for effective measures against this problem to be investigated.

Unfortunately, sedimentation is a whole system of a problem that is difficult to accurately calculate and predict. Let alone that, all the solutions widely used to mitigate it are mostly temporary in nature: dredging, sluicing, flushing, usage of check dams to retain part of the inflowing sediment, etc. The question is whether it is worthwhile to engage in such short-term measures or if we should endeavor for something more permanent, that being the subject of this project, namely, Sediment Bypass Tunnels(SBTs).

The answer to that is not that simple, but, as with many things dam-related, it mostly comes down to cost and benefit. The main issue with SBTs is that their cost does not simply amount to the cost of construction of a long tunnel often through difficult terrain. Instead, SBTs come with a sizeable annual maintenance expense, because sediment flowing through a tunnel can be and is quite destructive. As for

the benefits, first and foremost SBTs are the only permanent solution to the issue of sedimentation. Once placed they have the potential to divert nearly the entirety of inflowing sediment. That is why they should be preferably built parallel to the construction of a new dam so that the reservoir of said dam might never experience sedimentation in the first place. That said, SBTs can always be built for existing dams. Moreover, a sediment bypass tunnel doesn't solely remove sediment. Instead, it transports it back into the main river flow downstream of the dam in a constant manner quite alike to how it would be transported if the dam did not exist in the first place. This is of major use in the prevention of erosion of the river ecosystem downstream and is even more important in the cases of river deltas near lakes and seas, which suffer the most from lack of sediment transported from upstream.

With all the above in mind, it becomes clear that SBTs are the most effective solution to the problem of sedimentation and thus the equation that must still be solved is in regards to cost reduction. In that regard, the design and construction costs of the tunnel itself are, at a base level, dependent upon the decision between a short or a long diversion tunnel. A short diversion tunnel, or, better said, a diversion tunnel whose entrance is somewhere within the bounds of the reservoir, is obviously much cheaper to build but suffers from a higher rate of destruction and requires careful operation in order to facilitate sediment diversion in an acceptable manner.

On the other hand, a tunnel whose entry point is at the entrance or before the entrance to a dam's reservoir will be of a significant construction cost due to its sheer length. At the same time, such a long tunnel requires a lot less supervision to function adequately and is cheaper to maintain. Whichever of the two options is chosen however, the construction cost will still be noticeably high though that is no different to similar works concerning dams, such as fish ladders or a dam itself.

Therefore, the main goal, and the final objective of this project, should be to predict the annual cost of maintenance of a sediment bypass tunnel due to damages caused by the diverted sediment, a cost which, in turn, will be the main indicator of the overall usefulness of a sediment bypass tunnel especially when seen in comparison to other sediment control measures.

Of course, calculating this annual expense requires a lengthy analysis that must start from a basic input point, that being the rainfall, and eventually moving all the way to the volume of construction material lost per annum from the sediment bypass tunnel. To better observe this whole process, it has been split into the following five parts with each one of those being represented by one of the chapters of this technical essay:

- Rainfall IDF Curve Methodology for Regular Rainfalls
- Determination of Rainfall Limits for Sedimentation
- Calculation of Yearly Sedimentation via R.U.S.L.E
- Creation of a Tunnel Flow Model
- Calculation of Tunnel Material Loss due to Sediment Flow

In order for those parts to be more constructively presented, they will be viewed via a hypothetical example which is the reservoir of the Ladonas dam in the region of Arcadia in Greece. Essentially the various calculations have been conducted for the case of a sediment bypass tunnel operating for that specific area of interest and hence with the input data of that area specifically. Be that as it may, the process is only presented through this area of interest as an example without being specific to that dam's situation as it is constructed in such a way that makes it applicable in other potential cases also.

1.2 Project Outline

Based on what was just mentioned in 1.1 the decision was made to split this text into the following chapters:

- Chapter One: Introduction and General Information
- Chapter Two: Area of Interest – Ladonas Dam Reservoir
- Chapter Three: Rainfall IDF Curve Methodology for Regular Rainfalls
- Chapter Four: Determination of Rainfall Limits for Sedimentation
- Chapter Five: Calculation of Yearly Sedimentation via R.U.S.L.E
- Chapter Six: Creation of a Tunnel Flow Model
- Chapter Seven: Calculation of Tunnel Material Loss due to Sediment Flow
- Chapter Eight: Conclusions and further research

Chapter 2 - Area of Interest – Ladonas Dam Reservoir



Figure 1: View of the Ladonas Dam

The Ladonas dam and its hydro-electric power plant was constructed in 1955 and is located in the region of Arcadia, within the municipality of Gortynia and more specifically within the municipal units of Kleitor, Kontovazaina and Tropaia. It stands at 42 m of height from its base at 380 m to its dam crest at 422.4 m and has a maximum reservoir volume and surface area of 47.85 hm³ and 4.31 km² respectively at full capacity which is at a height of 420 m. Its installed capacity stands at 70 MW.

In regards to this project in particular, the selection of the Ladonas reservoir as the site under whose scope a potential sediment bypass tunnel would be viewed, was not by chance. Sedimentation within the Ladonas reservoir has become a growing issue recently especially as the dam enters its seventh decade of existence. The

point of interest is therefore whether the rainfall data combined with R.U.S.L.E. would paint a similar picture and if a sediment bypass tunnel would be viable in terms of its annual repair cost in that specific location.

However, to calculate the repair costs, the construction material of the sediment bypass tunnel must be first established. There are two options in this regard: 1) reinforced concrete, 2) granite. The selection between the two depends largely on the predominant form of destruction caused by the flowing sediment. If the grains are mostly saltating then reinforced concrete is the most optimal option whereas if they are mostly rolling then it is granite. By default, and in most river beds, particles are mostly saltating rather than rolling or sliding and that was what was assumed in this project also and hence reinforced concrete was chosen for the tunnel invert of this project. Moreover, granite would be a difficult and highly expensive option. Granite would need be mined near the dam site else it must be transported there in tiles, the latter of which would be the case for the Ladonas dam. Therefore, construction costs and future repair costs would become exorbitant due to the procurement and transportation costs of the material itself. In contrast the expense for the production, supply and placement of reinforced concrete is relatively low.

Last but not least, a choice must be made in regards to the length of the tunnel or, more precisely, whether the entrance to it will be within the reservoir or at the reservoir head. Should the entrance be within the reservoir then the tunnel can be of significantly smaller length and thus lower construction cost but will require much more careful management as the reservoir must be emptied to below the level of the tunnel's entrance prior to a storm else it will not function at all. On the other hand, if the entrance of the tunnel is at the head of the reservoir, then all incoming sediment will be always diverted and without the need for constant monitoring of the reservoir level for that to happen. In general, and whilst more expensive initially, a longer tunnel is much less risk-prone and will function without fail and thus it was what was chosen for this project.

Chapter 3 – Rainfall IDF Curve Methodology for Regular Rainfalls

In order for sedimentation to even be calculated in the first place, rainfall data are required. More precisely hourly or 30-minute rainfall data need to be available as sedimentation only occurs: a) above a threshold of total event rainfall, b) above a rainfall peak and c) if the rainfall event is not interrupted, or in simpler words if it does not start, end and then continue again. The margins for these three limits will be determined in the next chapter of this project. The problem now is that rainfall data within the area of interest are at best available for daily rainfall and thus a methodology is required to split such rainfall into individual steps which can then be compared against the limits mentioned previously.

The method chosen for this endeavour are the rainfall IDF curves through which flood event rainfall is calculated based on a number of parameters, the step of the rainfall calculations and the basin area based on the return period of the event. The difference here is that the method will be used backwards. Instead of creating a rainfall based on the return period of an event, the return period will be found based on a known rainfall.

Essentially what is known is the daily rainfall from the data of two stations close to the Ladonas dam, “ΔΑΦΝΗ(747)” and “ΠΑΓΚΡΑΤΑΙΚΑ ΚΑΛΥΒΙΑ(766)” which in turn was extracted from the data publicly available on hydroscope[1]. The first step here is to find the weight of the measurements of the two stations and that is noted as w_i in the calculations. w_i is found via a split of the basin area into two Thiessen polygons on arcmap with the Thiessen polygon tool existing within that program. The basin surface area is found by using the watershed tool of arcmap on a dem file of Southern Greece itself downloaded from the SRTM 90m DEM Digital Elevation Database[2]. The second step is to find the surface factor ϕ of the last step of the rainfall. That is calculated based on the basin surface area, A , and the step k of the last step which is equal to the total duration of the rainfall event, or 24 hours in this case. The calculation of ϕ is achieved from the following equation:

$\varphi = \max \left\{ 1 - \frac{0.048A^{0.36-0.01\ln A}}{k^{0.35}}, 0.25 \right\}$	Eq. 1 [3] , [4,1]
--	---

Then using the known weights, w_i , the actual total daily rainfall in mm, $H_{total,d,obs}$, is found via multiplication of the rainfall value given by each station with their respective w_i and then by adding up those results. In order to force even more conservative results on the final measurements, if one of the two stations did not have data for a specific day or had recorded zero rainfall but the other station had recorded a non-zero rainfall on the same day then the non-zero recording was assumed as the final rainfall as is and without multiplying with that station's weight.

The total rainfall in mm that resulted from the aforementioned process and for every single observation day is shown in the following diagram:

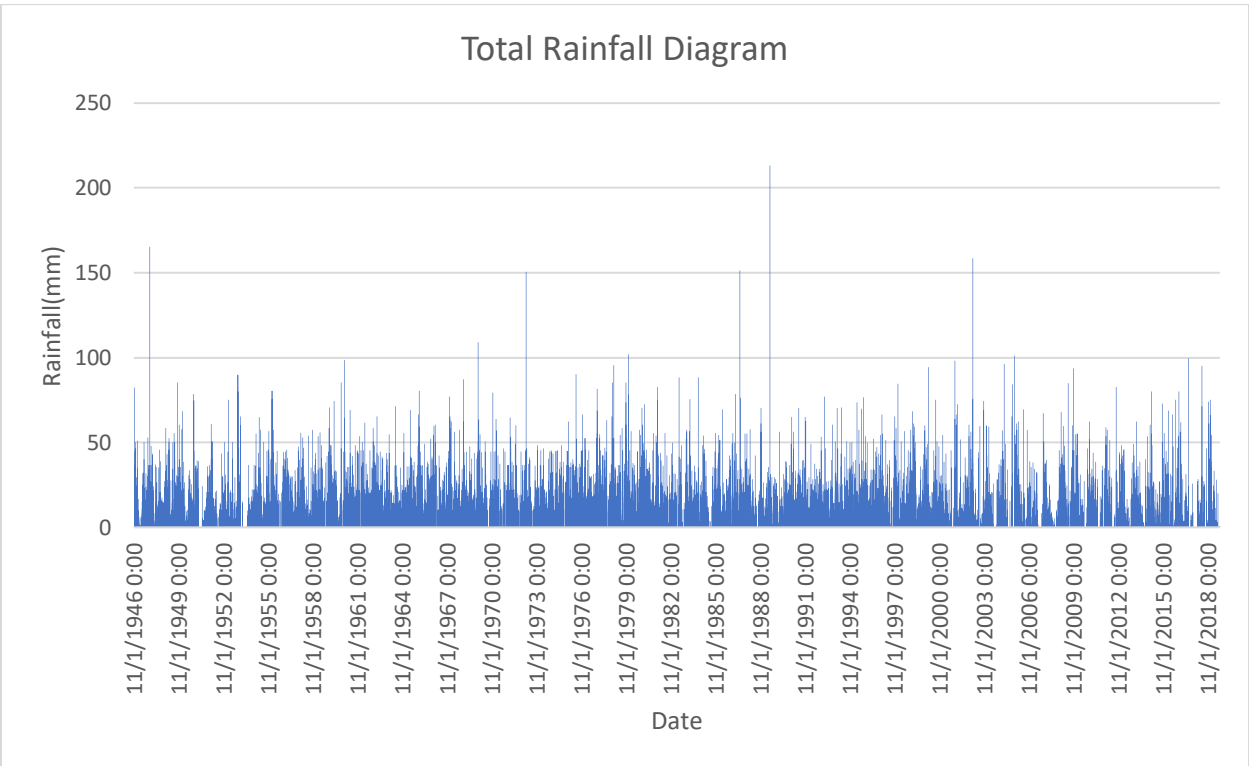


Figure 2: Total Daily Rainfall in mm at the Ladonas subbasin based on observations and weight of stations 747 and 766

The final total daily rainfall was then turned into the last step total hourly rainfall in mm/h, $H_{total,last}$, of that same day via division of the actual total daily rainfall

by ϕ times the time of the last step in hours. The last step is essentially the total duration of the rainfall event. In the final calculations a step of 2.4 hours was assumed with an event length of 24 hours in total and thus the time of the last step is 24 hours.

At this point we can find the return period of the rainfall event. We have the following equation which finds the rainfall x in mm/h based on a number of parameters, α , λ , β , ξ and η [4,3], the time of the step k in hours and the return period, T in years.

$x = \lambda_* \frac{(T/\beta_*)^\xi - 1}{(1 + k/\alpha)^{\eta_*}}$	Eq. 2 [4,2]
---	--------------------------------

The goal here is to solve the above for the return period. The last step total hourly rainfall will thus be the calculated x and thus k equals the time of the last step, or 24 hours in this case. However, before that, we require the parameters α , λ , β , ξ and η . Now α and ξ both have a set value of 0.18. To find λ , β and η we first require the polygon data of those parameters from the site of ΥΠΕΚΑ. Once we have those, we load them into arcmap and then clip them based on the watershed drawn previously. We then use the attribute tables of our clips to find the weighted averages of those values, which is calculated by the sum of each value multiplied by the area it occupies and that divided by the total area. The weighted average of each parameter is what will be used for λ , β and η . Knowing all necessary values we then solve the aforementioned equation for T and we find the return period of each daily rainfall.

Once we have found the return period, T , of every rainfall we use that return period along with the parameters we found and use the same equation to split the daily rainfall into steps, which in this case are 2.4 hours long each. Then by subtracting from every step the value of the previous one we find the rainfall that fell during that step specifically. We then multiply that rainfall with the ϕ of that step based on eq. 1 in order to receive the amount of rainfall distributed across the basin area and that is, per 2.4-hour step, the rainfall value that we need so as to facilitate the calculations for the sedimentation in the reservoir.

Chapter 4 – Determination of Rainfall Limits for Sedimentation

Having established the methodology through which the daily rainfall observations can be split into 2.4-hour steps of 24-hour events, we can now determine which rainfall events will cause sedimentation and which will not. That is done based on the requirements of R.U.S.L.E. for sedimentation to occur which have been mentioned at the start of chapter 3. More specifically the limits stated by R.U.S.L.E. are^[5]:

1. Total event rainfall of at least 12.7 mm
2. A rainfall peak of at least 12.7 mm if each event step is 30 minutes or 6.35 mm if each event step is 15 minutes
3. A total rainfall of less than 1.27 mm during a 6-hour time frame splits two consecutive events

Criterion 3 cannot be applied on the model of this project as the available data provides daily rainfall and the split into rainfall steps is artificial and not observed. Thus, checking if there is such a six hour gap with very little rain between days with successive rainfalls is pointless as the rainfall length, 24-hours in this project, is purely an assumption used to facilitate the artificial splitting of said daily rainfall into individual, 2.4-hour in this project, steps. In other words, it is impossible to know the rainfall event length just with the daily rainfall data and therefore it is equally impossible to figure out whether the rainfall observed the next day is a continuation of the rainfall that started the previous day or an entirely new rainfall event.

Criterion 1 represents total event rainfall, which in this project is equivalent to total daily rainfall since the event length is assumed to always be 24 hours and thus it is used as is.

Criterion 2 cannot be applied as is. That is because of the rainfall step used, which is 2.4 hours long instead of 30 minutes or 15 minutes long which are the steps R.U.S.L.E. provides the previously mentioned limits for. The obvious question here is why a 30- or 15-minute step wasn't used so as to align with the limits provided by R.U.S.L.E. The answer to that has to do with the methodology described in chapter 3 itself. Rainfall IDF curves are designed by default to simulate a flood event rainfall. However, the daily rainfall data which are split with this method in

this project have in their vast majority not been observed during flood events but rather regular, short time, low intensity rainfalls. That is also the most significant issue with using the IDF curves as they are for this purpose: they were not designed for this task. To alleviate this problem and force the IDF curves to project non-flood rainfalls it is necessary to have a longer step as it causes the model to consolidate most of the rainfall amount within the first few steps as would be expected in such rainfalls with small return times.

Even so the method still has a major flaw as it assumes that both smaller and larger rainfalls have the exact same length which is simply not the case. A rainfall of a total of, for example, 20 mm will not last 24 hours but can possibly be as short as 2 hours. On the other hand, a rainfall of 100 mm can last 24 hours but both of them will be split evenly in this method. This in turn explains the rainfall peak chosen in this project which is 4.5 mm, less than even the 6.35 mm of a 15-minute step rainfall event. The idea behind the small peak limit is to consider smaller rainfalls which would create sediment flow but would not have otherwise been counted due to how they are arranged by the method of chapter 3. Via the combination of a longer step and a smaller peak limit the inclusion of all possible sedimentation events based on an artificial rainfall split is made possible without the possibility of exclusion of smaller rainfalls.

Of course, the whole process for the consideration of criterion 2 requires more research and data analysis for more accurate limits to be produced. Unfortunately, I do not possess the equipment with a processing power sufficient to accomplish that and this specific matter deserves an entire future project of its own.

All the above said, it is still necessary to acquire an indication of whether the combination of the methodology used to split the daily rainfall with the sedimentation limits applied lead to a reliable result. That indicator is the number of days per year during which sedimentation has occurred which is the same as the number of events/days during which criteria 1 and 2-since criterion 3 is not used-are fulfilled. In this project that number is calculated at 48.84 days per year. By comparison the Mud Mountain dam in the U.S. has about 83 erosion days observed in it per year [\[6\]](#). Thus, the number of erosion days calculated was of the expected scale and therefore the rainfalls that passed the two criteria checks used were considered acceptable for the calculation of the sedimentation.

Chapter 5 – Calculation of Yearly Sedimentation via R.U.S.L.E.

With the necessary rainfall data for the usage of R.U.S.L.E. obtained, the next step is to calculate the various factors of the R.U.S.L.E. model. Those can be obtained via already existing maps and diagrams but it was thought as more beneficial to go through the entire detailed process in this project. Whatever the case, the factors to be calculated are the following:

- 5.1 The rainfall erosivity factor, R
- 5.2 The soil erodibility factor, K
- 5.3 The topographic factor, LS
- 5.4 The land coverage factor, C
- 5.5 The erosion control/protection factor, P

5.1 The rainfall erosivity factor, R [7]

We will begin the process with the rainfall erosivity factor since that is tied directly to the rainfall data inputs. R is calculated from the following expression:

$R = \frac{1}{n} \sum_{j=1}^n \sum_{k=1}^{mj} (EI_{30})_k$	Eq. 3
--	-------

In eq. 3 R is calculated in (MJ mm ha⁻¹ h⁻¹ month⁻¹). However, due to the fact that each rainfall event is contained within one day and because of the fact that the data sheet is arrayed with daily rainfalls, it is both more accurate and more practical to find R directly as yearly rather than monthly and hence to calculate it in (MJ mm ha⁻¹ h⁻¹ year⁻¹). This also requires a change of eq. 3 as mj is no longer necessary. mj denotes the number of erosive events in one month. However, since the set function already excludes non-erosive days and the calculations are for an annual R, that is unnecessary. The calculations are conducted individually for each and every erosive day and they are then summed up before being divided by the total amount of observation years, which would be n in this case, which ultimately results in the annual R.

However, the calculation of this yearly R is still dependent on EI30 just like with a monthly R. EI30 is calculated as follows:

$EI_{30} = \left(\sum_{r=1}^m e_r v_r \right) I_{30}$	Eq. 4
--	-------

In eq. 4 v_r is the rainfall volume in mm during each time step of an event, or of a day in this project, and I_{30} is the maximum rainfall intensity in $\text{mm} \cdot \text{h}^{-1}$ during a 30-minute interval. That said, since the time step is 2.4 hours in this project, I_{30} is the maximum rainfall intensity during a 2.4-hour interval or, in other words, the rainfall intensity of the rainfall step that is the peak of the rainfall event. Then, e_r represents the unit rainfall energy in $\text{MJ} \cdot \text{ha}^{-1} \cdot \text{mm}^{-1}$ and is in turn calculated as follows:

$e_r = 0.29[1 - 0.72 \exp(-0.05i_r)]$	Eq. 5
---------------------------------------	-------

Here i_r is the rainfall intensity during each time step in $\text{mm} \cdot \text{h}^{-1}$. In this project in particular, $e_r \cdot v_r$ was found for every step of every daily rainfall, then the $e_r \cdot v_r$ of every step was summed up and that sum was multiplied by the I_{30} of that daily rainfall event. Then the results of that process gave the daily R whenever the rainfall was deemed erosive based on the criteria detailed in chapter 4. If that day's rain was not deemed erosive then the resulting EI30 was discarded for that day. Following that, all valid EI30 results were summed and their sum was then divided by the number of observation years, thus providing the average annual R in $\text{MJ} \cdot \text{mm} \cdot \text{ha}^{-1} \cdot \text{h}^{-1} \cdot \text{year}^{-1}$. In this project the annual R was found to be $904.71 \text{ MJ} \cdot \text{mm} \cdot \text{ha}^{-1} \cdot \text{h}^{-1} \cdot \text{year}^{-1}$ which is much higher than the R found in the closest station to the Ladonas reservoir, the station at Tropaia which has a recorded R of about $570 \text{ MJ} \cdot \text{mm} \cdot \text{ha}^{-1} \cdot \text{h}^{-1} \cdot \text{year}^{-1}$ [7,2]. However, $904.71 \text{ MJ} \cdot \text{mm} \cdot \text{ha}^{-1} \cdot \text{h}^{-1} \cdot \text{year}^{-1}$ is meant to be an R representative of the average R for the entire Ladonas watershed and when looking at the area covered by that watershed on the R-rainfall erosivity maps of the R.U.S.L.E. model we can see that said area contains regions with an R ranging from 500 to 1000 and with the majority of them being within areas with an R of 610 to 730 or 730 to 900 with a few areas being in the 900 to 1300 range in the western and southern parts of the subbasin of the dam. Due to that range of R coverage the calculated R of $904.71 \text{ MJ} \cdot \text{mm} \cdot \text{ha}^{-1} \cdot \text{h}^{-1}$

year-1 is fairly reasonable. The total observation years and the average yearly R are also shown in the table below:

Table 1: Total number of years with observed rainfalls and the average yearly R calculated from those

Total Years	72.11
Total(Average Yearly) R(MJ*mm/(ha*h*year))	904.71

The rainfall erosivity map referenced above is the following one:

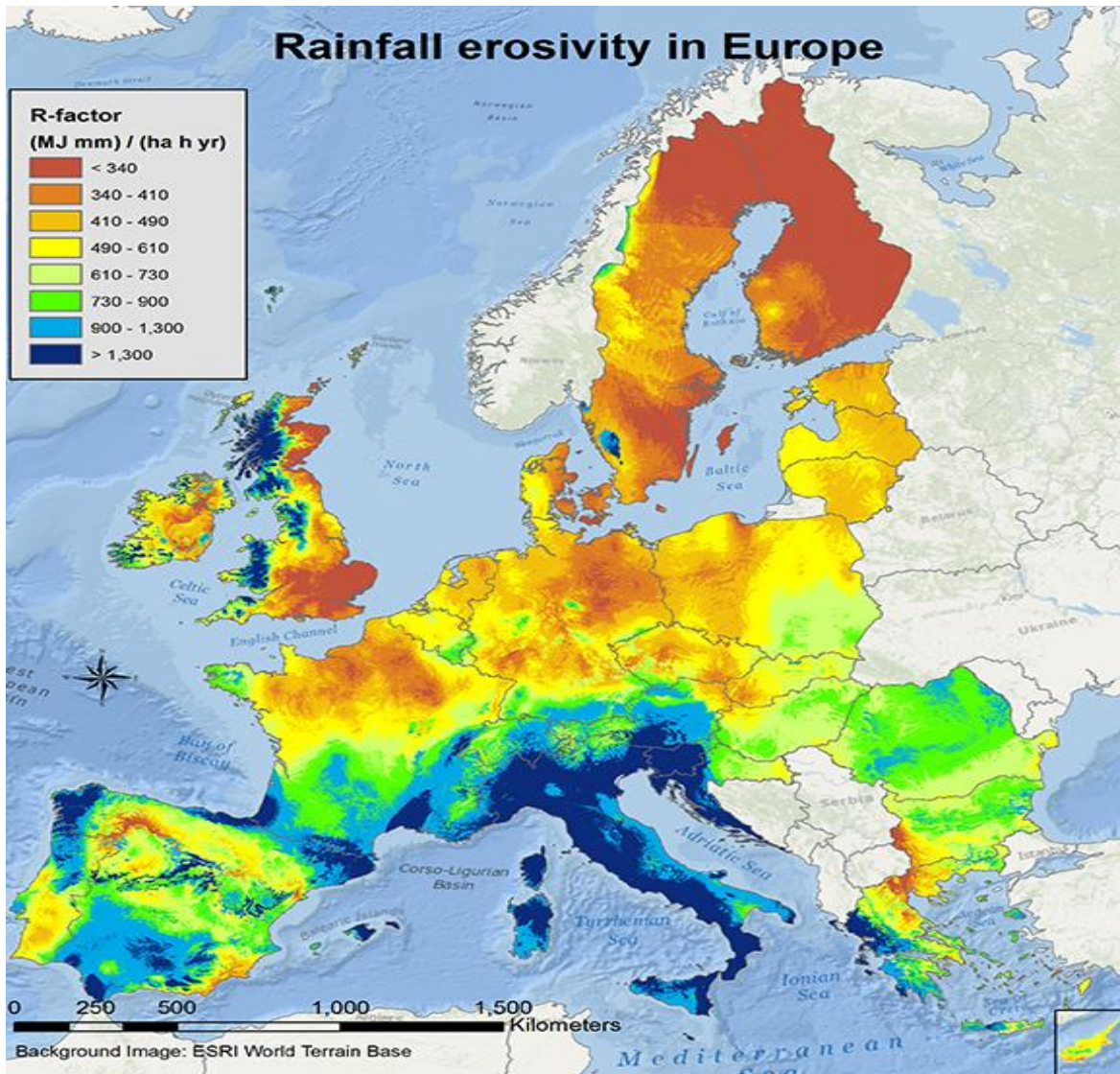


Figure 3: R-factor high resolution(2015)

5.2 The soil erodibility factor, K [8]

The soil erodibility factor is derived from the algebraic approximation proposed by Wischmeier and Smith (1978) and Renard et al. (1997) and which is based on five soil parameters namely the texture, the organic matter, the coarse fragments, the structure, and the permeability. The aforementioned equation is the following one:

$K = [(2.1 \times 10^{-4} M^{1.14} (12 - OM) + 3.25 (s - 2) + 2.5 (p - 3)) / 100] * 0.1317$	Eq. 6
---	-------

In eq. 6 we have the following values:

- M, the textural factor which is equal to the fraction of silt content(msilt(%)) plus the fraction of very fine sand content(mvfs(%)) and then that multiplied by 100 minus the fraction of clay content(mc(%)).
- OM(%), the percentage of organic matter in the soil
- s, the structure class of the soil which comes in 4 categories: s=1: very fine granular, s=2: fine granular, s=3, medium or coarse granular and s=4: blocky, platy or massive
- p, the permeability class whose lowest value is 1, meaning very rapid flow/high permeability, and whose highest value is 6, meaning very slow flow/low permeability.

To find the textural factor M what we need to know are the contents of the soil in silt, very fine sand and clay. Clay are grains with an average diameter of less than 0.002 mm, silt with 0.002 to 0.05 mm and very fine sand with 0.05 to 0.1 mm. A hydrologic soil group map was obtained from NASA's open data portal[9] and was then cut down to the outline of the watershed already created previously on arcmap. Within the cut map only the hydrological groups C and D existed with but a few dots being of group D. Thus, the total percentage of HGC-C to the total coverage was calculated and that was roughly 99.88%. Category D would lower the amount of very fine sand and raise the amount of clay and thus the calculations were adjusted based on the percentage of HGC-C to the total coverage by multiplying the fine sand percentages of HGC-C, 45%, with the aforementioned percentage 99.88% and then adding 100-99.88% to the clay percentage of HGC-C, 30%. Notably 30% is the average of the extreme ends of possibly clay percentage in HGC-C which are 20 and 40%. Afterwards the final

percentages of clay and fine sand were added and then subtracted from 100 thus outputting the percentage of silt within the soil as it is the intermediate kind of soil between clay and very fine sand. In the end there was 30.035% of clay, 25.018% of silt and 44.947% of very fine sand. This in turn results in an M equal to 4895.058.

The organic matter content was obtained from the “Organic Matter in the Soils of Southern Europe” by Pandi Zdrrouli, Robert J. A. Jones and Luca Montanarella [\[10\]](#). More specifically figure 4 of that report shows the organic carbon content of southern Europe and for the area of interest we can observe that it is exclusively within the low organic carbon category, or, in other words, the area of interest has $OC < 2\%$. This in turn means that the topsoil has low ($< 2\%$) or very low ($< 1\%$) organic carbon. In turn $OC \leq 1\%$ means $OM \leq 1.7\%$ and $OC \leq 2\%$ means $OM \leq 3.4\%$. Given the lack of any more detailed data sets for the watershed for the area of interest of this project, an OM of 3% was assumed in this case as it is neither too low nor too high a figure and it is, in any case, within the low OC category.

For s an estimation was made based on the region where the watershed is located, that being the mountainous part of northern Arcadia. With that in mind, s was set to a value of 2 meaning a soil structure that is fine granular.

For the permeability class, p, and as we can observe from the percentages of clay, silt and very fine sand noted previously, the soil within the area of interest has a texture which can be categorized as being between a loam and a sandy loam texture. That conclusion comes from the fact that there is more sand than clay and silt but at the same time the amount of clay is comparable and slightly higher than the amount of silt. A sandy loam texture has a $p = 2.5$ whilst a loam texture has a $p = 1.3$ [\[11\]](#). Considering that the amount of sand is still quite higher than the amount of clay, the texture is probably closer to a sandy loam texture than to a loam one and thus an intermediate value closer to that of a sandy loam was selected and that value was $p = 2$.

Last but not least and since Ladonas is a dam in Greece which in turn is a Mediterranean country, the stoniness of the ground must also be considered since it plays a major role in the reduction of soil erosion in southern European countries. The average reduction in soil erosion due to stoniness in southern Europe is estimated at 15% and that is the reduction assumed within this project

also. With all the above in mind the final K factor has been calculated to be 0.031 which is fairly reasonable for the Ladonas watershed since that area is in the regions of 0.02-0.028 and 0.028-0.033 on the R.U.S.L.E. K-factor map. The overall values and parameters of the aforementioned calculations can be seen in the following table:

Table 2: K-factor calculation table

Kst(Correction of K factor due to Stoniness)(Average Reduction in %)	15.00%	
A(km ²)	793.87	
km ² to mi ²	0.39	
A(mi ²)	306.43	
ps(t/m ³)	1.6	
SDR	0.21	
Balance towards HSG-C	1.00	
Clay Fraction Content(<0.002 mm)	mc(%)	30.04
Silt Fraction Content(0.002-0.05 mm)	msilt(%)	25.02
Very Fine Sand Fraction Content(0.05-0.1 mm)	mvfs(%)	44.95
Textural Factor	M	4895.06
Organic Matter Content	OM(%)	3
Soil Structure Class(1:very fine granular-4:blocky,platy or massive)	s	2
Permeability Class(1:very rapid-6:very slow)	p	2
Soil Erodibility((t*ha*h)/(ha*MJ*mm))	K	0.031

The R.U.S.L.E. K-factor maps with and without stoniness taken into consideration can be seen below and in the next page:

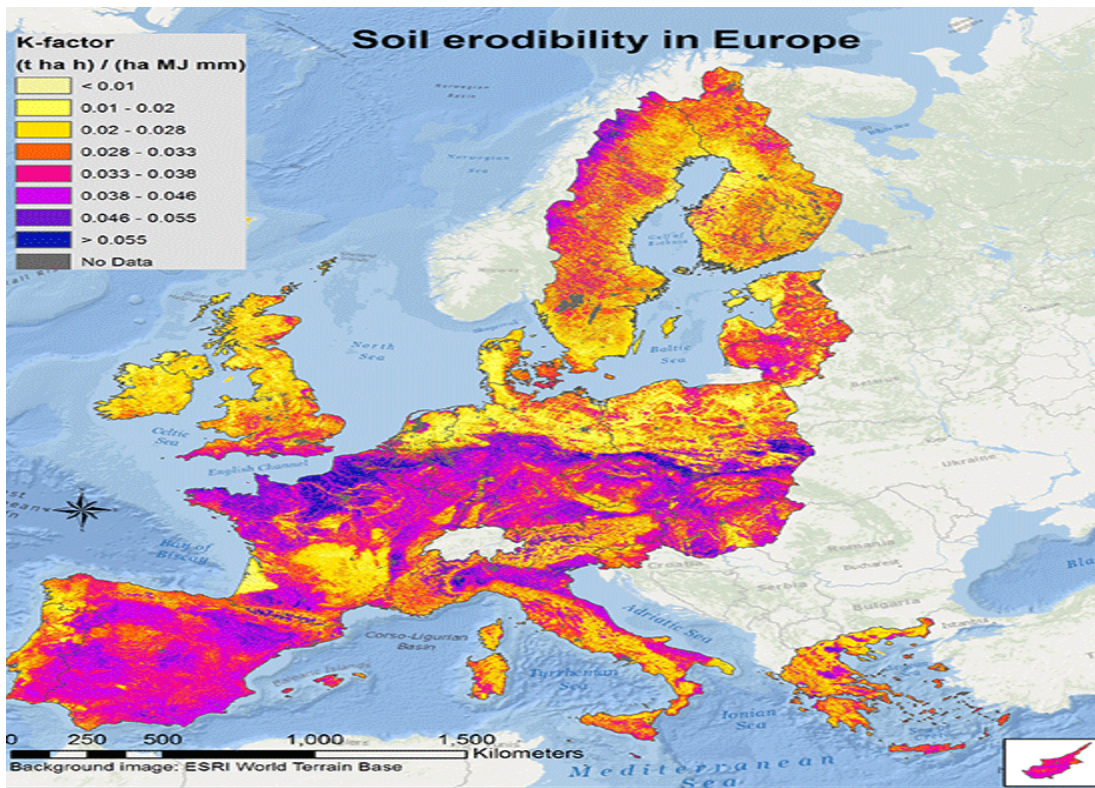


Figure 4: K-factor high resolution(2014) (Without stoniness)

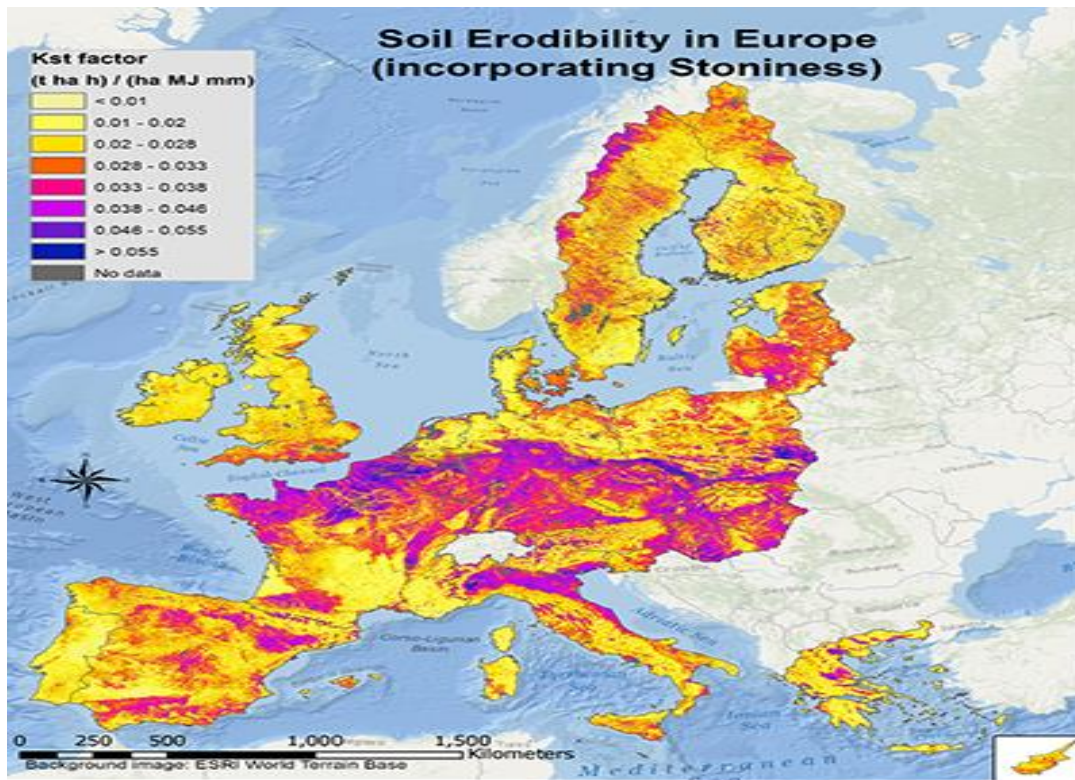


Figure 5: K-factor incorporating Stoniness

5.3 The topographic factor, LS [12]

As the abbreviation for this factor suggests LS is a multiplication of L times S where L is the average length of the slope within the watershed and S is the average gradient of the slope within that same watershed. In turn L is derived from the following equation:

$L = \left(\frac{\lambda}{22.13} \right)^m$	Eq. 7
--	-------

In eq. 7 λ is the weighted slope length and m is a factor dependent upon the weighted slope s in %. In particular, m is equal to 0.5 if $s \geq 5\%$ or 0.4 if $s = 3$ to 4% or 0.3 if $s = 1$ to 3% or 0.2 if $s < 1\%$. For the calculation of λ the slope length tool of arcmap was used for the area of the watershed. Then the results were extracted into an excel sheet. The results include a slope length column and a column with the amount of cells that contain each slope length. Then a third column is created that calculates the multiplication of the values of the previous two columns. The

sum of that third column divided by the sum of the second column is the weighted average of the slope length in meters.

For the slope $s(\%)$ the slope tool of arcmap was used and the resulting values were processed in excel in the exact same way as with the slope length. The resulting value for the slope however is in degrees. That value is then translated to radians before its tangent is found and that is divided by the tangent of 45 degrees in radians and the result of that is multiplied by 100 thus giving us the weighted slope in %. In this project the calculations yielded a slope length of 16.72 m and a slope of 22.18% and thus m is equal to 0.5 since s is over 5%. With m and λ known, eq. 7 was used and the resulting L was 0.87. Last but not least the slope gradient factor is calculated from the following equation:

$S = \frac{0.43 + 0.3s + 0.043s^2}{6.574}$	Eq. 8 [13]
--	-------------------------------

In this project and using eq. 8 S was found to be equal to 4.30. After multiplying L and S the resulting LS is equal to 3.736 which is a fairly reasonable number since it is close to the average LS for Greece which is 3.79 and it also is within the range of 3 to 5 which is characteristic for the region around the Ladonas dam based on the R.U.S.L.E. LS factor map. All results regarding the LS -factor can also be viewed in the table below:

Table 3: LS-factor calculation table

LS(Greek Average)	Ls	3.79
λ (length of slope)(m)	16.72	
m (factor due to slope)	0.5	
L (Slope-length factor)	0.87	
Mean s (Slope)(%)	22.18	
S (Slope-gradient factor)	4.30	
LS (topographic factor)	3.74	

The R.U.S.L.E. LS factor map can be seen in the next page:

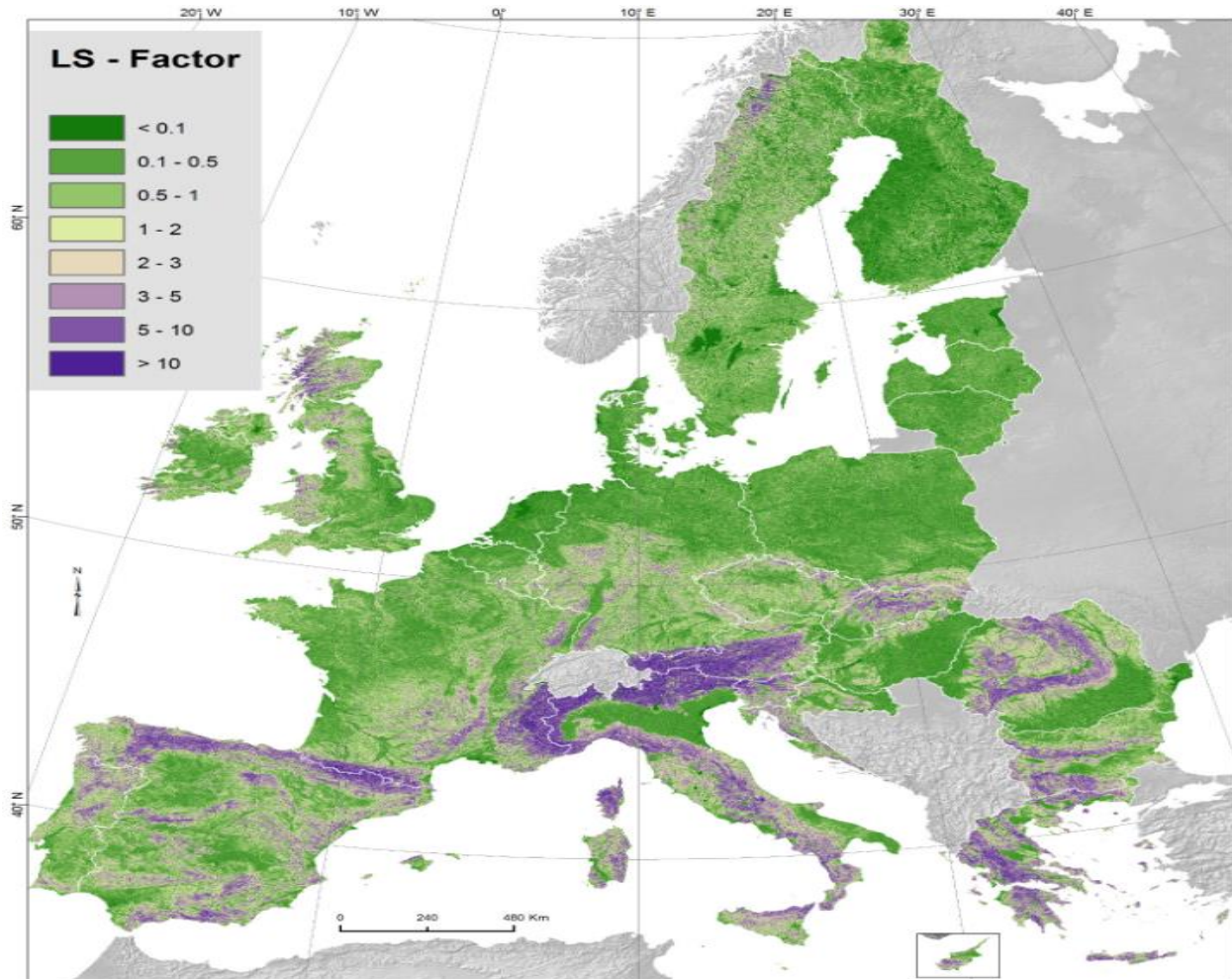


Figure 6: Slope length and steepness factor (LS-factor) in the European Union

[5.4 The land coverage factor, C \[14\]](#)

The first consideration for factor C is whether the land in question is arable or not. The issue here is that the watershed of the Ladonas dam contains both arable and non-arable land. Once a C_{arable} and a $C_{non-arable}$ have been calculated, a weighted average based on the coverage of each kind over the entire watershed is created. That weighted average is the factor C that will be used in the R.U.S.L.E. calculations of this project.

To calculate the C_{arable} , the coverage and kind of the crops cultivated within the Ladonas watershed must be known and whilst there is no data for the Ladonas watershed in particular, there is enough data for the region of Arcadia within

which the Ladonas watershed is located. Unfortunately, the R.U.S.L.E. model crop categories do not include all possible kinds of crops or rather, they are general categories whilst the available data denotes crop plants individually by their scientific latin names. Therefore, each and every crop plant has to first be matched to one of the categories of the R.U.S.L.E. model. The R.U.S.L.E. categories have been condensed into the following table where all categories with the same Ccrop are placed in the same line.

Table 4: Crop Categories Reference Chart

Crop Categories Reference Chart		
Number	Type	Ccrop
1	Rice	0.15
2	Common wheat and spelt - Durum Wheat - Rye	0.2
3	Barley	0.21
4	Linseed	0.25
5	Oilseeds - Soya	0.28
6	Rape and turnip rape	0.3
7	Dried pulses (legumes) and protein crop - Sunflower Seeds	0.32
8	Potatoes - Sugar Beet	0.34
9	Grain maize – corn	0.38
10	Tobacco	0.49
11	Cotton seed - Fallow Land	0.5
12	Other(Grapevine-Vineyard)	0.3

The crops found in Arcadia have been obtained from the genesys database [\[15\]](#) and have been matched to the most suitable category(Cat. No.) of the above table as shown in the following tables. These tables also include the number of accessions (Amount column) that each crop kind was found being cultivated in as well as the percentage of that amount to the total number of recorded accessions (Amount(%) column). Last but not least the corresponding Ccrop of each crop kind based on the category that each crop was matched to is also listed.

Table 5a: Kinds of crops in Arcadia and corresponding Ccrop numbers, a: Cereals, grasses

Cereals, grasses	Amount	Cat. No.	Amount(%)	Ccrop
Aegilops comosa Sm.	3	2	1.62	0.2
Aegilops lorentii Hochst.	2	2	1.08	0.2
Aegilops triuncialis L.	1	2	0.54	0.2
Dactylis glomerata L.	4	3	2.16	0.21
Festuca arundinacea Schred.	1	1	0.54	0.15
Haynaldia villosa (L.) Schur.	1	2	0.54	0.2
Hordeum bulbosum L.	1	3	0.54	0.21
Lolium perenne L.	5	2	2.70	0.2
Lolium sp.	1	2	0.54	0.2
Triticum aestivum L.	3	2	1.62	0.2
Triticum durum Desf.	2	2	1.08	0.2
Zea mays L.	34	2	18.38	0.2
Subtotal	58			

Table 5b: Kinds of crops in Arcadia and corresponding Ccrop numbers, b: Pulses and other legumes

Pulses and other legumes	Amount	Cat. No.	Amount(%)	Ccrop
Cicer arietinum L.	11	7	5.95	0.32
Lathyrus sativus L.	4	7	2.16	0.32
Lens culinaris Medik.	14	7	7.57	0.32
Lens esculenta Moench.	1	7	0.54	0.32
Medicago coronata (L.) Bartal.	1	7	0.54	0.32
Medicago orbicularis (L.) Bartal.	3	7	1.62	0.32
Medicago sp.	4	7	2.16	0.32
Medicago truncatula Gaertn.	2	7	1.08	0.32
Phaseolus vulgaris L.	3	7	1.62	0.32
Trifolium alexandrinum L.	3	7	1.62	0.32
Trifolium repens L.	3	7	1.62	0.32
Vicia ervilia (L.) Willd.	4	7	2.16	0.32
Vicia faba L.	8	7	4.32	0.32
Vicia sativa L.	13	7	7.03	0.32
Vicia sativa L. subsp. Sativa	2	7	1.08	0.32
Vicia sativa L. subsp. sativa var. obovata Ser.	1	7	0.54	0.32
Subtotal	77			

Table 5c: Kinds of crops in Arcadia and corresponding Ccrop numbers, c: Vegetables and wild edibles, Other crops, Full Total Amount of Accessions recorded

Vegetables and wild edibles	Amount	Cat. No.	Amount(%)	Ccrop
Brassica cretica Lam.	4	6	2.16	0.3
Lactuca serriola L.	2	8	1.08	0.34
Brassica cretica Lam. subsp. laconica Gustafs. and Snogerup.	1	6	0.54	0.3
Subtotal	7			
Other	Amount	Cat. No.	Amount(%)	Ccrop
Grapevines	43	12	23.24	0.3
Subtotal	43			
Full Total	185			

At this point it should be noted that an accession does not translate directly to any specific area coverage. That said all accessions have been assumed to be of the same or similar size and thus the percentage of each crop based on the number of accessions it was found in was then used to find the coverage of each crop by multiplying the percentage amount of accessions of each crop with the total surface area covered by arable land within the Ladonas subbasin. The determination of the surface area covered by arable land will be explained in the calculation of $C_{non-arable}$ as it is essentially the entire subbasin area minus the non-arable area within that subbasin.

However, for the calculation of a general C_{crop} for the region of Arcadia, the knowledge of the area coverage is not necessary. The basic calculation of C_{arable} is simply a multiplication of C_{crop} by $C_{management}$.

$C_{management}$ is a condensation of the various agricultural practices which can control the amount of erosion within agricultural land. More specifically that reduction can be due to tillage practices, plant residues and/or cover crops. A multiplication of the three factors, $C_{tillage}$, $C_{residues}$ and C_{cover} , leads to the final $C_{management}$.

For $C_{tillage}$ we must consider the tillage practices used in the region.

Unfortunately, there is no data for the agricultural areas within the Ladonas subbasin. The R.U.S.L.E. $C_{tillage}$ map indicates a reduction of C of 22% to 30% due to tillage practices for the region of Arcadia. However, that's most likely inapplicable to the largely mountainous subbasin of the Ladonas dam. Instead, a worst case scenario was assumed and standard conventional tillage practices were assumed and hence $C_{tillage}$ was set to 1.

Next up, the plant residues again cannot be found for the Ladonas subbasin itself as there are no data specific to that region. However, a correlation between the crop kinds and whether or not they have residues can be made. In particular, pulses and legumes have no residues or have very few residues. Everything else, or in other words cereals, grasses, vegetables, wild edibles and grapevines, have at least some residues. Since it had been previously assumed that the same average C_{crop} would be used for all of Arcadia, that means that all over-arching crop categories have been hypothesized to be relatively evenly distributed in the entirety of Arcadia. By that logic the plant residues caused by those crop

categories would also be distributed in the same way and hence the average Cresidues that is calculated for Arcadia will also apply to the Ladonas subbasin. The average Cresidues is 0.88 for the R.U.S.L.E. model and thus the function for its calculation is as follows:

$C_{\text{residues}} = (0.88 \times F_{\text{residues}}) + (1 - F_{\text{residues}})$	Eq. 9
---	-------

In the above function, F_{residues} denotes the amount of arable land that is affected by plant residues. In this project, that would be the land covered by cereals, grasses, vegetables, wild edibles and grapevines. Note that here F_{residues} is the sum of the percentage amounts (Amount(%)) of coverage for each category divided with 100. In the end, the final result is a Cresidues of 0.93 which translates to a 7% reduction of factor C, which is fairly reasonable considering that the R.U.S.L.E. map for Cresidues shows that the region of Arcadia has a reduction of factor C due plant residues of over 4%.

Then for C_{cover} , and due to lack of data on the usage or not of cover crops within the Ladonas subbasin, the same consideration with C_{tillage} was made, that cover crops are either not used at all or their use is minimal owing largely to the fact that the region is very mountainous. Thus, C_{cover} was set at 1 meaning that cover crops are not used in the Ladonas subbasin or their use is so infrequent that it can be considered negligible. This ensures that the worst-case scenario is assumed for the region as that is the safest option due to the lack of any cover crop data for the subbasin.

The multiplication of the aforementioned values of C_{tillage} , C_{residues} and C_{cover} leads to a $C_{\text{management}}$ of 0.93.

$C_{\text{crop,arable}}$ is a simple average value of all C_{crop} based on each crop's coverage percentage. Thus, it is calculated by multiplying the C_{crop} of each crop kind-which is in turn found based on the category it belongs to which was established previously-with the coverage percentage of that crop kind, then adding the results of that multiplication from all crop kinds and dividing them by 100. The resulting value in this project is 0.28.

To find the final Carable, and as mentioned previously, we simply multiply Ccrop,arable with Cmanagement and in this project the resulting value is roughly 0.26. The overall results in regards to Carable can be seen in the table below:

Table 6: Carable calculation table

Calculation of C factor	
C-Crop,arable	0.277
C-Management	
Ctillage	1
Cresidues	0.930
Ccover	1
C-Management	0.930
Carable	0.258

Next the Cnon-arable is required. Unfortunately, there is no data for the Ladonas subbasin or for region of Arcadia that specifically shows which land masses are specifically arable and which are not. That said, using the ESRI land coverage map we can deduct roughly which areas are arable and which aren't. In particular for the Ladonas subbasin we have the following land coverage categories:

1. Water
2. Forest(Trees)
3. Agricultural(Crops)
4. Medium Density Residential(Built)
5. Open Spaces(Bare)
6. Snow/Ice
7. Grasslands/Pasture(Range)

From the above categories, agricultural and residential land have been considered arable land in their entirety in this project. For agricultural land that was done for the obvious reason that most agricultural land is arable else it would be noted as a grassland. For residential land the R.U.S.L.E. model distinguishes no separate Clanduse, which is the equivalent to Ccrop for arable land. Thus, either a relatively high Clanduse should be assumed or that land should use Carable as that is significantly high to begin with. Considering that most residential land is near the agricultural one and that using a high Clanduse would still mean using a high but ultimately random number, Carable was used for the residential land despite that land being neither arable or non-arable in reality.

The main issue here are grasslands and pastures. Intuitively most land that is such is non-arable because it would be noted as agricultural otherwise. However, it is also likely that crops that are either below ground, like many pulses and legumes, as well as low lying crops of grasses, like trifolium, which are most definitely arable crops, might be viewed as grasslands or pastures when viewed from a satellite which is precisely the kind of data ESRI provides. Therefore, considering the previously mentioned possibility but also knowing that all actual pastures and grasslands are non-arable, the surface area noted under the grasslands and pastures category was split in half with one half being considered arable and the other non-arable.

All other land coverage types, namely water, forests, bare open spaces and snow and ice, are obviously non-arable. Each one of these categories was assigned a suitable Clanduse based on its most fitting category from the R.U.S.L.E. model. Water was assigned a Clanduse of 0 since it obviously does not represent land and hence cannot be considered for the calculation of the land coverage factor. Snow and ice cover were assigned the Clanduse of glaciers and perpetual snow which is 0. For forest cover the worst possible Clanduse for forests was chosen which is 0.003. Open bare space was given a Clanduse of 0.275 which is the average of the extreme Clanduse values for sparsely vegetated areas which have a Clanduse of 0.1 to 0.45. Last but not least, the non-arable part of grasslands and pastures was assigned the average Clanduse for pastures which is 0.1 as pastures have a Clanduse which ranges between 0.05 and 0.15.

To calculate Cnon-arable all we need to do is create a weighted average of the previous Clanduse of each non-arable land coverage kind. That is done by multiplying the surface area of each non-arable land coverage type with its Clanduse, summing up the results of those multiplications and then dividing that result by the total non-arable surface area. The end result of this process is a Cnon-arable of roughly 0.034.

At this point we have both a Carable and Cnon-arable each corresponding to the arable and non-arable surface area of the Ladonas subbasin respectively. The arable surface area is found simply by deducting the non-arable surface area from the total one. It should be noted here that Carable was not directly calculated based on this arable surface area contrary to Cnon-arable. Instead, and as

explained previously, Carable was calculated based on a number of accessions. However, since the accessions are of the same or similar size, we can assume that the total land coverage of the crop accessions is equal to the arable surface area found here. With that out of the way, all we have to do is find the weighted average of Carable and Cnon-arable by multiplying each one with their corresponding surface area, adding the resulting values and then dividing that sum by the total subbasin surface area. The result of that process is the C factor and, in this project, it has been calculated at roughly 0.095. That value is fairly reasonable as, according to the R.U.S.L.E. cover-management factor(C-factor) map, the Ladonas subbasin includes regions with C-factors of 0.03-0.07, 0.07-0.1 and 0.1-0.15. The overall calculations in regards to Cnon-arable and the final C-factor can be seen in the following three tables:

Table 7a: C-factor calculation table, a: Land coverage types and corresponding Cnon-arable numbers

Cnon-arable*Non-arable Area	Cnon-arable per type	Area(km2)	Land Coverage Type
0	0		4 Water
1.167	0.003		389 Forest(Trees)
0	0.35		24 Agricultural(Crops)
0	0.45		12 Medium Density Residential(Built)
0	0.275		0 Open Spaces(Bare)
0	0		0 Snow/Ice
18.25	0.1		365 Grasslands/Pasture(Range)
			794 <- Total Area(km2)

Table 7b: C-factor calculation table, b: Land coverage types and determination of those as arable, non-arable, partly arable

Land Coverage Type	Numbers=Percentage of Non-arable in Total	Non-Arable Area(km2)
Water	Non-arable	4
Forest(Trees)	Non-arable	389
Agricultural(Crops)	Arable	0
Medium Density Residential(Built)	Arable	0
Open Spaces(Bare)	Non-arable	0
Snow/Ice	Non-arable	0
Grasslands/Pasture(Range)	0.5	182.5

Table 7c: C-factor calculation table, c: Final C-factor, Ctotal, calculation

794 <- Total Area(km2)	Total Non-Arable Area(km2) ->	575.5
	Total Arable Area(km2) ->	218.5
	Cnon-arable	0.034
	Ctotal	0.095

The R.U.S.L.E. C-factor map can be seen below:

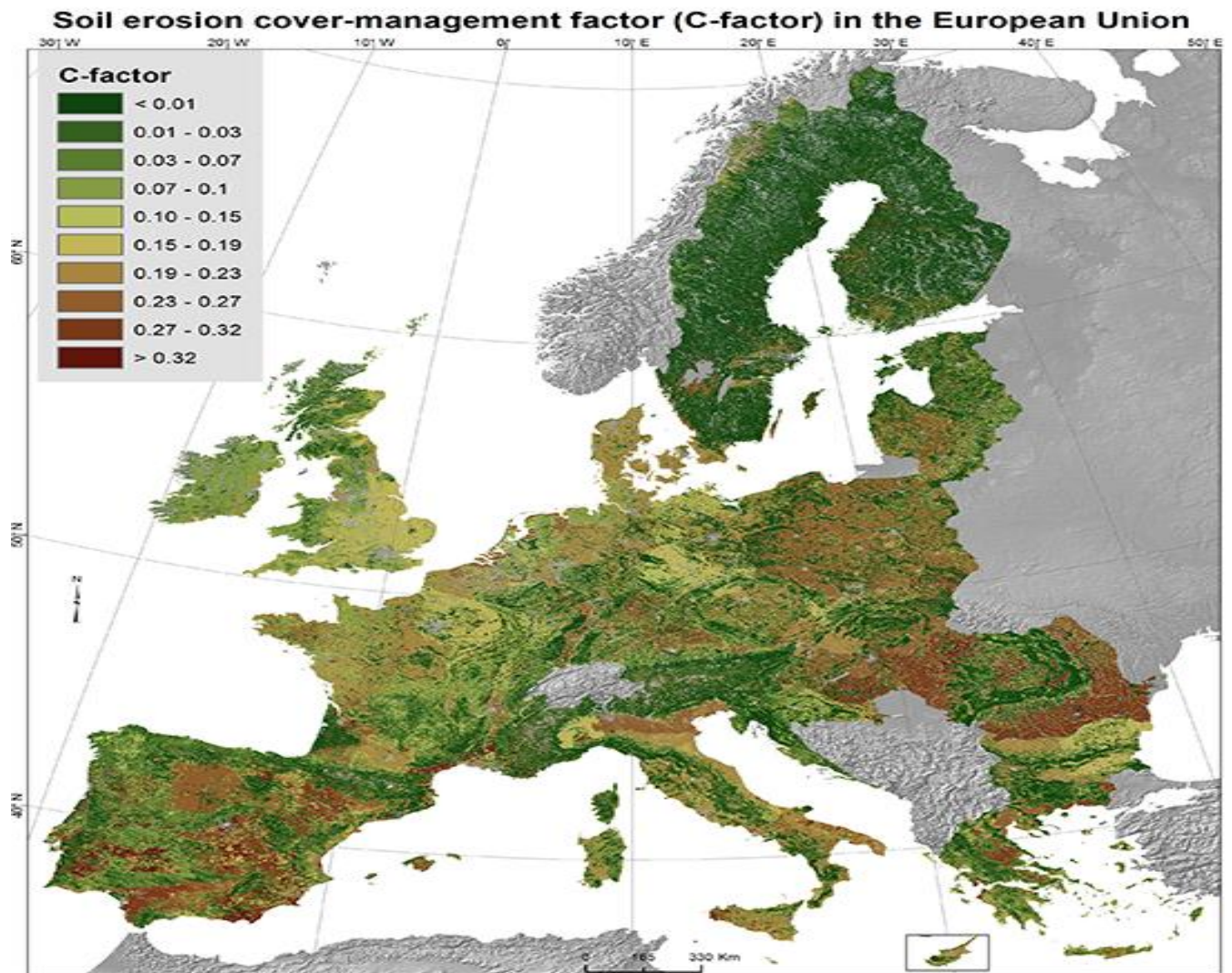


Figure 7: C-factor map of the European Union

[5.5 The erosion control/protection factor, P \[16\]](#)

The subbasin of the Ladonas dam is a generally mountainous and forested region with a small number of settlements. Judging by that fact alone, it is hard to believe that there would be any erosion control measures in place in the region. Therefore, the erosion control/protection factor P was set to a value of 1 meaning that no practices are present in the region. And, indeed, if one looks at the Support conservation practices factor (P-factor) in the European Union map the

entire Ladonas subbasin is greyed out meaning that there are no conservational practices active in the area.

Table 8: P-factor calculation table

Measures for Erosion Control	
P	1 1 = no conservational practices

The R.U.S.L.E. support practices map can be seen below:

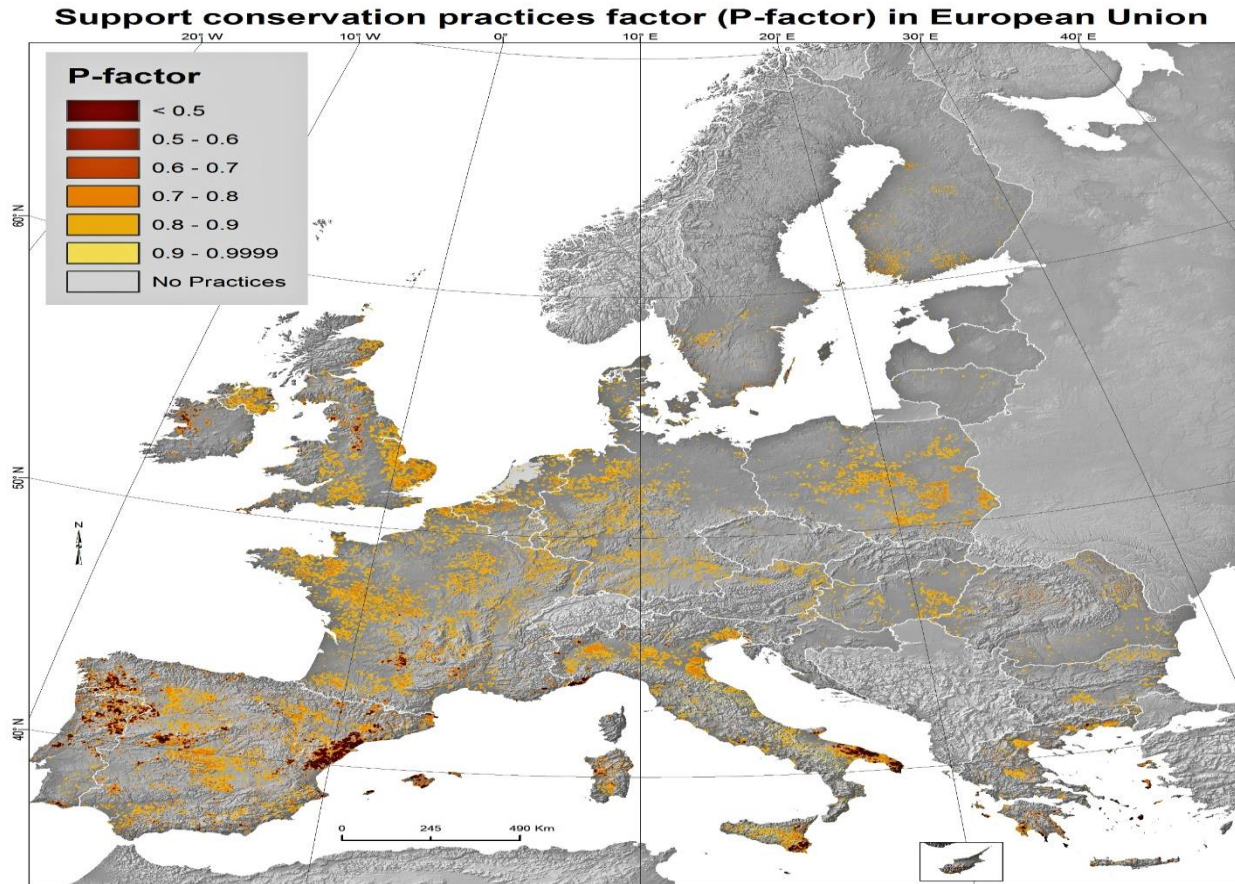


Figure 8: Modelling the effect of support practices (P-factor) on the reduction of soil erosion by water at European Scale

5.6 Calculation of sediment volume

At this stage all of the required factors for the calculation of soil loss of each daily rainfall event are known. The soil loss of each event is thus easily calculated as the result of the R factor of each rainfall event times the factors K, LS, C and P which were explained previously. However, it must be noted here that the R.U.S.L.E.

model under-evaluates the R-factor by 20%[\[7,3\]](#). Due to that the previous result will be multiplied by a safety factor of 1.2 and that will give us the final soil loss in t/ha for each erosive rainfall event.

Of course, the soil loss in t/ha isn't extremely useful as a number. The value that we are looking for is the sediment volume per day/event in hm³. To find that we will use the following equation which translates soil loss to soil loss distributed across a surface area A:

$V = \rho \text{ SDR } L A$	Eq. 10 [17]
-----------------------------	--------------------------------

In eq. 10 ρ is the density of the sediment, ρ_s , which in this project has been set to 1.6 t/m³ but can generally be anything between 1 to 1.6 t/m³. 1.6 t/m³ has been assumed here as it is the worst-case scenario. Then, L is the soil loss which we calculated previously and A is the surface area over which the soil loss will be distributed, which in this case is the Ladonas subbasin which is equal to 793.87 km². SDR is a dimensionless factor which shows the amount of soil that gets trapped in the exit of the subbasin and it is calculated from the following equation:

$\text{SDR} = 0.42 A^{-0.125}$	Eq. 11 [17,2]
--------------------------------	----------------------------------

It should be noted here that in eq. 11 the surface area A is in mi² and not km² and therefore the subbasin area should be converted to mi² in order for SDR to be calculated. At any rate, the resulting SDR for the Ladonas subbasin is equal to 0.205. With these inputs we find the sediment volume in hm³ based on eq. 10 for each day/event. The resulting average yearly sedimentation is 0.103 hm³. This in turn translates to a sedimentation percentage of about 15.4% of the total volume of the Ladonas reservoir during this year, 2024. At the 100-year mark from the opening of the Ladonas dam the sedimentation of the reservoir will be at 22.3% of the total reservoir volume. That means there is quite a significant problem of sedimentation in the Ladonas reservoir and therefore the construction of a Sediment Bypass Tunnel is justified as it is an effective and permanent solution for such cases where the rate of sedimentation is high. As an extra note the annual rate of sedimentation of the Ladonas reservoir is about 0.22% of the total reservoir volume which is indeed significant.

The table below shows the aforementioned results as well as the average yearly soil loss-which is the immediate result calculated by R.U.S.L.E.-in t/ha:

Table 8: Final Sedimentation Results Table

	Sedimentation Time X(years)	Total Reservoir Volume(hm3)
	69	46
	Sedimentation Volume in X years(hm3)	Percentage of Sediment to Total Volume in X years(%)
	7.081651581	15.39489474
	Sedimentation Volume in 100 years(hm3)	Percentage of Sediment to Total Volume in 100 years(%)
	10.26326316	22.31144165
Average Yearly Soil Loss(t/ha)	Average Yearly Sedimentation(hm3)	Percentage of Sediment to Total Volume per year(%)
0.802973738	0.102632632	0.223114417

The graph below shows the 200 days during whose rainfalls the highest daily sedimentation was observed:

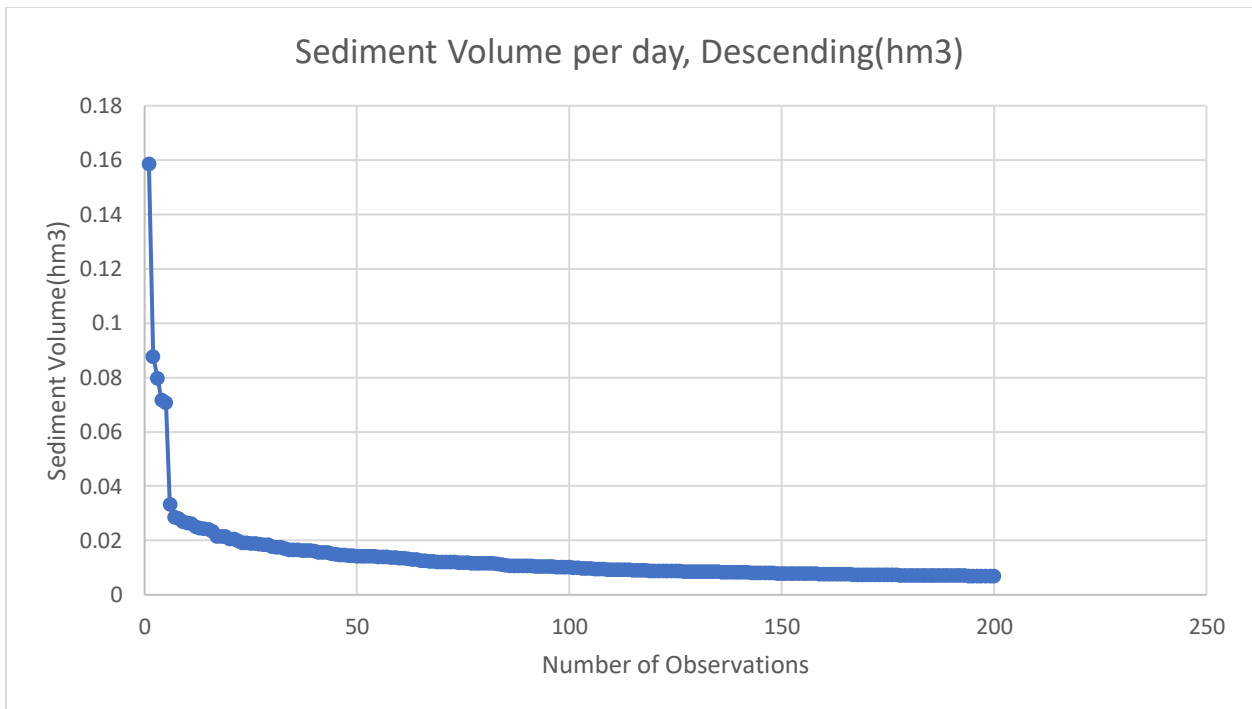


Figure 9: The 200 most “sediment-carrying” daily rainfalls

Chapter 6 – Creation of a Tunnel Flow Model

Since the sedimentation rate of the Ladonas reservoir justifies the creation of a Sediment Bypass Tunnel, the issue is thus whether a sediment bypass tunnel is a viable option financially or if other methods for the management of the incoming sediment should be examined. Of course, and as explained in chapter 2, the problem is not the construction cost as any sedimentation measures-much like any significant supplementary dam works-are bound to be expensive to implement. Instead, the issue is the significant repair cost for the damages that the sediment bypass tunnel will incur during its operation.

6.1 Creation of a rainfall event input

In order to estimate the cost of the damages, the first step is to create a tunnel flow model showing how the water of an incoming rainfall flows through the sediment bypass tunnel. The first point to consider for such a model is which the input rainfall should be. Based on the data gathered in chapter 5 it might be tempting to use the average erosive rainfall for this purpose, which in this case measures at about 27.09 mm of total rainfall with a return period of 0.63 years. The problem with such an option lies in the method that is used to turn such an average erosive rainfall into a rainfall event with small time steps and in particular 30-minute steps in this project. That is because the method used for this are the rainfall IDF curves which, as explained in chapter 3, do not function very well with low return periods. Even when used directly and not in the opposite manner in which they were used in chapter 3, rainfall IDF curves still have this particular issue.

To circumvent this issue a very simple consideration was made: the input rainfall would be a flood rainfall, or, in other words, a 100-year return period rainfall, and then the results would be adjusted to project an average erosive rainfall event. The rainfall IDF curves are applied normally and in a direct manner with a T equal to 100. The method functions just fine with such large-scale return periods and thus no more adjustments are necessary.

The question now is how such a flood event will be adjusted to project an average one. For that we need to ask: what is absolutely known about both a 100-year

event and the average 0.63-year event? The answer is the total event rainfall, a number that is characteristic to the two rainfalls also. It is equal to 27.09 mm for the 0.63-year event and 158.03 mm for the 100-year event. To turn any final value that has come from an input of the 100-year rainfall into an average one all we have to do is multiply it by the ratio of the total average erosive rainfall to the total flood rainfall. With the data of this project that were stated just before, this ratio is equal to 0.171 or in other words an average erosive rainfall is 17.1% of a 100-year flood rainfall and consequently we assume that any final results of an average rainfall are likewise 17.1% of those derived from a flood rainfall. Granted such a hypothesis is far from perfect. In a perfect scenario, a methodology would be used that correctly translates small return-periods into 30-minute step rainfall events. However, absence of such a method, this assumption with the aforementioned ratio is a decent enough estimation.

The next problem is that the rainfall event itself is not an entirely useful piece of information in on itself for the purposes of measuring water flow through the sediment bypass tunnel. For that purpose, we need to translate the rainfall into outflow at the edge of the subbasin, or in other words at the reservoir. To accomplish that we need to pass the rainfall input through a HEC-HMS model which will then provide us with the required outflow table at the reservoir. Therefore, after creating a basic basin model in HEC-HMS we need to find the curve number and lag time of the subbasin. The process for the curve number has been partially stated already in chapter 5 as the ESRI map used for the distinction of arable and non-arable land is the one that will be used to determine the curve number. However, after downloading the coverage map for the region of southern Greece from ESRI and cutting it down to the extent of the Ladonas subbasin, we must now determine what curve number each land coverage type should have. For that purpose, the following chart which has been comprised of data from NRCS TR-55 and Halley et al. 2000 – ESRI Proceedings [\[18\]](#) has been used:

Table 10: Curve Number(CN) table based on corresponding land uses and hydrologic soil groups

Land Use Description	Cover Description		Hydrologic Soil Group			
	Cover Type and Hydrologic Condition	% Impervious Areas	A	B	C	D
Agricultural	Row Crops - <u>Staight</u> Rows + Crop Residue Cover- Good Condition (1)		64	75	82	85
Commercial	Urban Districts: <u>Commerical</u> and Business	85	89	92	94	95
Forest	<u>Woods</u> (2) - Good Condition		30	55	70	77
Grass/Pasture	Pasture, Grassland, or <u>Range</u> (3) - Good Condition		39	61	74	80
Herbaceous	Mixture of grass, weeds, brush – Good Condition		–	62	74	85
Shrubs	Thick and low shrubs – Good Condition		–	30	41	48
Disturbed/Transitional	Gravel parking, quarries, land under development		76	85	89	91
Industrial	Urban district: Industrial	72	81	88	91	93
High Density Residential	Residential districts by average lot size: 1/8 acre or less; Multi-family, apartments, condos, etc.	65	77	85	90	92
Medium Density Residential	Residential districts by average lot size: 1/4 acre to 1 acre; single-family	30	57	72	81	86
Low Density Residential	Residential districts by average lot size: 1 acre lot or greater; single-family	15	48	66	78	83
Open Spaces	Open Space (lawns, parks, golf courses, cemeteries, etc.) Fair Condition (grass cover 50% to 70%) (Open Space in Good Condition would have same CN as Grass/Pasture)		49	69	79	84
Parking and Paved Spaces	Impervious areas: Paved parking lots, roofs, driveways, etc. (excluding right-of-way)	100	98	98	98	98
Residential 1/8 acre	Residential districts by average lot size: 1/8 acre or less	65	77	85	90	92
Residential 1/4 acre	Residential districts by average lot size: 1/4 acre	38	61	75	83	87
Residential 1/3 acre	Residential districts by average lot size: 1/3 acre	30	57	72	81	86
Residential 1/2 acre	Residential districts by average lot size: 1/2 acre	25	54	70	80	85
Residential 1 acre	Residential districts by average lot size: 1 acre	20	51	68	79	84
Residential 2 acres	Residential districts by average lot size: 2 <u>acre</u>	12	46	65	77	82
Water			100	100	100	100

Within arcmap and in the attribute table of the clip of the land coverage map we note the names of each land coverage group and their corresponding curve number in two new columns. The same attribute table we are editing should already contain the surface area that each category covers. Therefore, we add yet another column to that table which will be set to the value of the curve number of each category multiplied by the surface area covered by that same category. Once that is complete, we extract the data of that column as well as the data of the surface area column onto excel as follows:

Table 11: Calculation table for Curve Number(CN)

From ArcMap	Ladonas
CNi*Area	400
	27230
	1968
	972
	0
	0
	27010
SUM	57580
Area	4 Water
	389 Forest(Trees)
	24 Agricultural(Crops)
	12 Medium Density Residential(Built)
	0 Open Spaces(Bare)
	0 Snow/Ice
	365 Grasslands/Pasture(Range)
SUM	794

Then we simply use the following weighted average equation which is the very same one we have already used for other parameters previously. This equation for CN is as follows:

$$CN = \frac{\sum_i^n CN_i \times A_i}{\sum_i^n A_i}$$

Eq. 12

Based on the above equation we find that CN, after being rounded up, equals 73. Next, we require the initial abstraction which in turn is equal to 5% of the maximum potential abstraction. To find the maximum potential abstraction, S, we apply the following equation.

$$S = 254 * (100 / (CN - 1))$$

Eq. 13
[\[20\]](#)

From eq. 13 we find that S is equal to 352.78 mm and thus the initial abstraction ha0 is equal to 17.64 mm. The last piece of data required in order to run the basin model on HEC-HMS is the lag time. Technically the first step here is to determine whether the method we'd need to use for that time is Muskingum or Lag time.

However, since the Ladonas subbasin is within a mountainous area the slope is bound to be quite high and Muskingum is only applicable for slopes of less than 1%. And indeed, in chapter 5 when calculating the LS-factor we had also calculated the slope to be 22.18% which is definitely a lot higher than 0.1%. Then the lag time is calculated as per the NRCS Lag time method which is shown in the following picture[19]:

- **8. NRCS Lag Time Method**

According to **NEH Part 630 Hydrology**, the NRCS Lag Time Method (**Figure 19**) is suitable for different watershed conditions ranging from heavily forested watersheds with steep channels and a high percent of the runoff resulting from subsurface flow, to meadows providing a high retardance to surface runoff, to smooth land surfaces and large paved areas. The curve number CN used in the equations should NOT be less than 50, or greater than 95.

$$T_l = \frac{L^{0.8} \left(\frac{1000}{CN} - 9 \right)^{0.7}}{1900S^{0.5}}$$

Where:

T_l = lag time (hrs)

L = longest hydraulic length of the watershed (ft)

CN = average watershed curve number

S = average watershed slope (%)

Assume *Lag time* = 0.6 x TOC,

$$TOC = \frac{L^{0.8} \left(\frac{1000}{CN} - 9 \right)^{0.7}}{1140 S^{0.5}}$$

Figure 10: NRCS Lag Time Method

Here we can see that to use this method the curve number must be between 50 and 95 but the curve number in this project is 73 and thus the method can indeed be used. In order to use the above method though we first need to find the longest hydraulic length of the watershed in ft, L. That information is easily obtained from arcmap by using the measure tool to check the length of the longest path in the flow accumulation layer of the watershed. The resulting L found was roughly 52182 m or 171200 ft. Thus, we can calculate TOC as shown

above based on the previously calculated CN, S and L and we find that TOC equals 8.46 hours. By multiplying that with 0.6 we find that the lag time is equal to 5.08 hours or 304.51 minutes. A summary of the results in regards to the curve number and the lag time is shown in the table below:

Table 12: Calculation table for initial abstraction, ha_0 , lag time and longest hydraulic length of watershed, l

CN _{middle}	72.52
Cn _{middle,roundup}	73
S(mm)	352.78
ha ₀ (mm)	17.64
S(inch)	13.89
l(m)	52181.80
l(feet)	171200.13
TOC(h)	8.46
Lag or Muskingum?	Lag
LagTime(h)	5.08
LagTime(min)	304.51

We then go to HEC-HMS and create the following basin model:

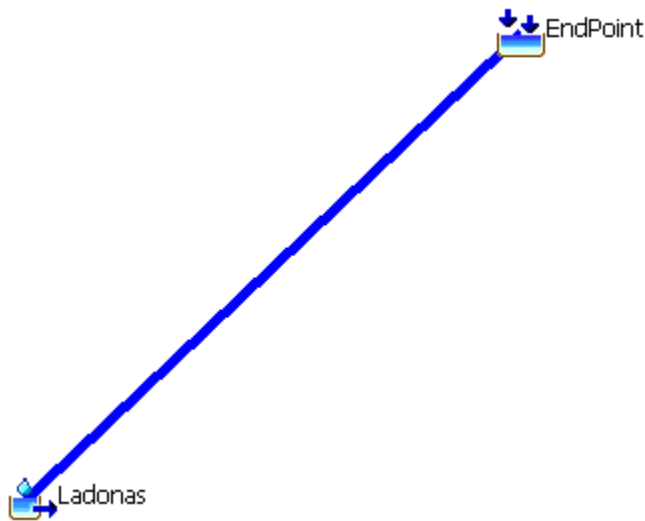


Figure 11: HEC-HMS basic basin model for the Ladonas subbasin

We then input the CN, lag time, initial abstraction and subbasin surface area as required and then input the rainfall event we created previously into a time series that's part of a gauge which is then connected to the meteorological model within

HEC-HMS. Specifically, the rainfall event that is inputted is the one shown in the following diagram:

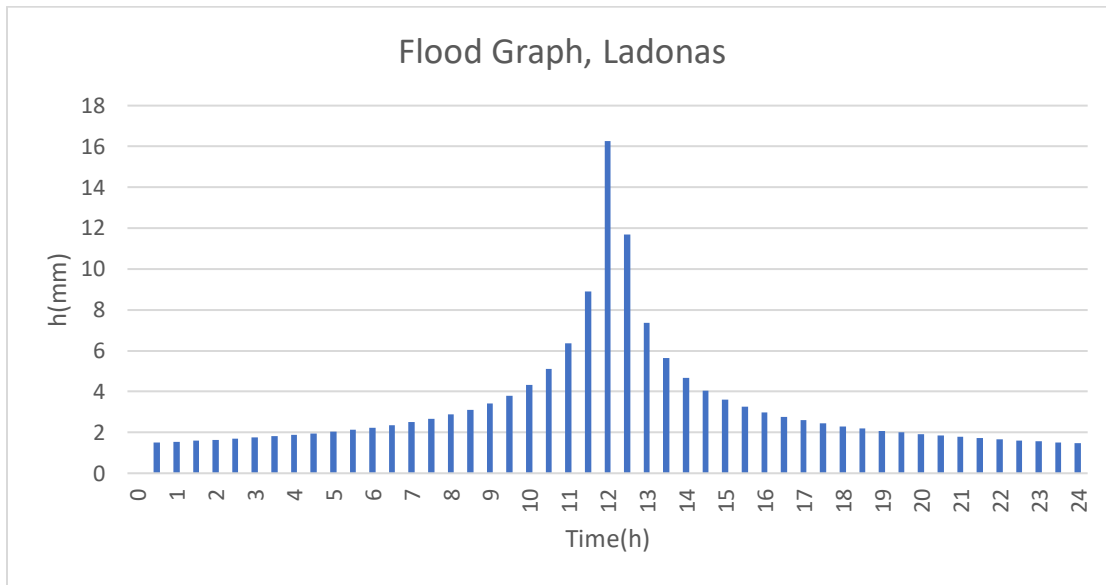


Figure 12: Rainfall height to time diagram for 100-year return period flood event

After that we run the HEC-HMS model and receive the table with the final outflow in m³/s for the endpoint. The values of that table are the ones which we need to input as basic flow data into our tunnel flow model. Those values are shown in the form of a diagram below:

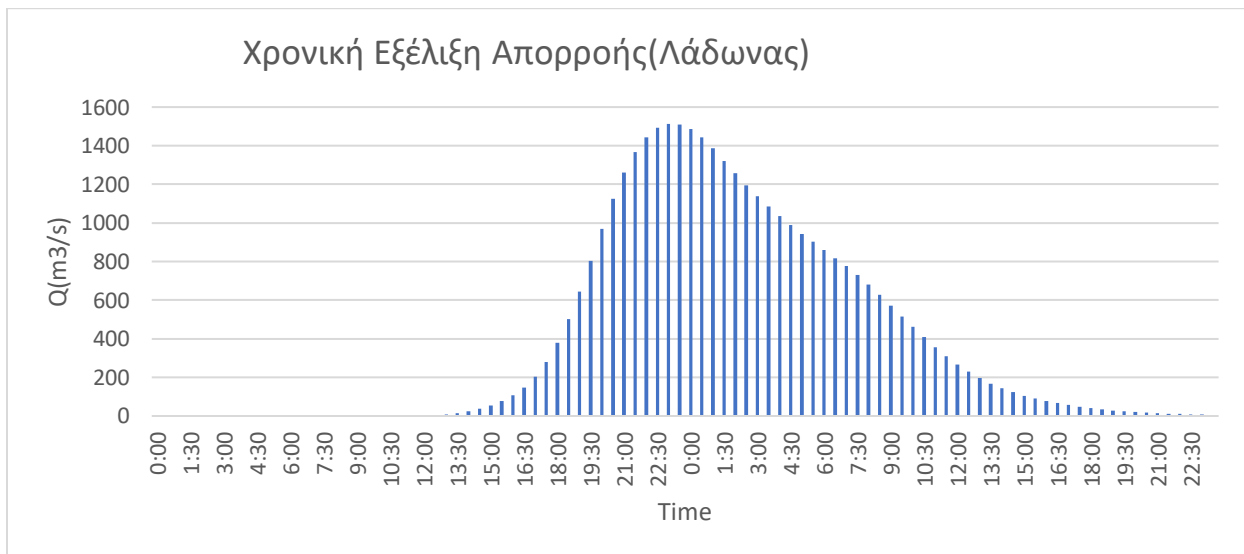


Figure 13: Water flow into the Ladonas reservoir of 100-year return period flood event

6.2 Height-volume equation parameters

The last piece of data required before we can begin constructing the tunnel flow model is the height-volume equation of the reservoir. It must be noted here that the height volume equation of the reservoir is only used in this project because the basin of the Ladonas reservoir has not been mapped out. This is important to note because sediment bypass tunnels are always built behind a weir which directs sediment towards the sediment bypass tunnel. The methods used for that vary but are beyond the scope of this project.

The important part to remember here is that the sediment bypass tunnel is behind a weir and usually close to the entrance of the reservoir as noted in chapters 1 and 2. That means that the water depths and volume that matter to the operation of a sediment bypass tunnel are those behind the weir and not those of the entire reservoir which in turn are the ones projected by the height-volume equation of the reservoir. That also means that the actual height-volume equation that should be used is that of the weir and not of the entire reservoir.

Unfortunately, since the basin of the Ladonas reservoir has not been mapped a height-volume equation cannot be constructed for anything other than the entire reservoir. The height-volume equation of the reservoir can be constructed because through the operation of the dam the height and volume of the reservoir at various points are known. On the other hand, behind the weir there exists a different correlation of height and volume.

One could argue here that since the weir is within the reservoir, its height-volume correlation would not differ all that much to the reservoir's. The problem with that lies with the second point brought up just before: this sediment bypass tunnel has been assumed with an entry point close to the entrance to the Ladonas reservoir. That means that the depth upstream from the weir and the sediment bypass tunnel is very low compared to the rest of the reservoir. To put this into perspective, the Ladonas reservoir has its bottom at 380 meters. However, the depth of the basin at the position chosen for the sediment bypass tunnel of this project is probably closer to that of the maximum reservoir height or, in other words, 420 meters. In this project and since the entrance of the sediment bypass tunnel is not directly at the entrance to the reservoir but instead a bit further within the reservoir, the base of the sediment bypass tunnel was set at 414

meters. The exact height of the bottom of the sediment bypass tunnel is impossible to predict accurately without data about the exact height of the reservoir basin at the position of the entrance of the tunnel. Due to that it might be necessary for the base of the tunnel to be moved further down in case the basin is at a height significantly lower than 414 meters.

As to why the height of 414 m was chosen, that is because of a number of satellite images available on google earth which show the bare reservoir basin at the area of the entrance of the tunnel. In those images, the height of the basin is noted at 412 m but that is most certainly a mathematical projection, given that the entire reservoir is shown as being at 412 m. However, what's probably more accurate is the height to the east of the bare reservoir area which is shown to be anywhere from 412 to 416 meters and based on that the middle value of 414 m was chosen. One of the aforementioned instances available on google earth where the dam basin is visible near the assumed position of a future sediment bypass tunnel is the one visible below:



Figure 14: Picture of the Ladonas reservoir east of the Pteria village (10/2022, Google Earth)

Here it should be noted that the tunnel bottom at the entrance can be slightly above the ground-floor but the difference must be as small as possible else the sediment might have trouble being funneled into the tunnel. That is important in this case especially since a system of a single sediment bypass tunnel is what is being proposed by this project. With a system of two sediment bypass tunnels, the larger tunnel must be close to the ground level but will only be operated during floods, with a smaller tunnel being the one that will be more frequently open. The smaller tunnel can be quite some height above the ground level and above the larger tunnel below as can be seen in the example of the Mud Mountain Dam which utilizes such a system of two sediment bypass tunnels [\[6,2\]](#).

With this parenthesis out of the way, the creation of a height-volume equation for the reservoir is done based on the equation type of $y=a*x^b$ where y is the volume in hm³ and x is the absolute height in meters. The volume of the reservoir in hm³ and surface area in km² for the various heights of the reservoir in meters as well as other accompanying basic data were provided by the professor who supervised this project, Professor Andreas Efstratiadis. The tables with this information are shown below and in the next page:

Table 13a: Ladonas dam data, a: Ladonas reservoir base height, dead volume, max reservoir level, dam crest, tailwater and installed capacity

Base z(m)	380.0
Dead volume (hm³)	400.0
Max pool level (m)	420.0
Dam crest	422.4
Tailwater (m)	372.0
Installed capacity (MW)	70.0

Table 13b: Ladonas dam data, b: Ladonas reservoir height, surface area and volume data

ΛΑΔΩΝΑΣ		
z(m)	Area (km2)	Volume (hm3)
380.0	0.00	0.00
383.0	0.29	0.68
385.6	0.29	1.34
388.7	0.48	2.12
391.0	0.49	3.43
392.6	0.75	4.42
393.9	0.75	5.52
395.5	0.75	6.95
398.3	0.75	8.70
400.6	1.10	10.79
402.3	1.22	12.66
403.4	1.22	14.52
404.7	1.22	15.84
406.2	1.22	17.81
407.8	1.22	19.57
409.6	1.22	21.54
411.2	1.49	23.73
412.5	1.49	25.93
414.1	1.49	28.56
415.3	3.04	30.53
416.0	3.60	33.05
416.6	3.60	36.12
417.7	3.60	38.86
418.0	3.80	40.83
418.6	3.80	43.02
419.3	3.87	45.44
420.1	4.31	47.85
420.5	4.31	50.59
420.8	4.31	53.00
421.7	4.32	55.84
422.4	4.32	58.15

Of course, the requirement here is the opposite of a height-volume equation, or, in other words, a volume-height equation. That is because the inputs of the tunnel flow model are flows in m³/s which will then be converted into water volume by multiplying with the time step of 0.5 hours every time. Then those water volumes need be converted into water height and that is the equation that we need.

Hence, we have:

$y = a \cdot x^b$ where y is volume in hm³ and x is height in m

and so

$$(y/a) = x^b$$

and so

$$(y/a)^{1/b} = x$$

and so

$$\left(\frac{1}{a}\right)^{\frac{1}{b}} * y^{\frac{1}{b}} = x$$

by setting $a = \left(\frac{1}{a}\right)^{\frac{1}{b}}$ and $b = \frac{1}{b}$ we have

$a * y^b = x$ though of course a and b are not the same to the ones from $y = a * x^b$

Granted we can use a and b from $y = a * x^b$ to calculate the a and b for $a * y^b = x$. However, this is not what was applied in this project. That is because the amount of decimal accuracy required for a and b is quite significant. Calculating a and b for $a * y^b = x$ in such an indirect manner will yield slightly inaccurate results and whilst the difference might seem minor, it ends up being quite important due to the amount of accuracy required in the volume-height equation. Thus, to calculate a and b for $a * y^b = x$ the following excel functions were used [\[21\]](#):

$$a = \text{EXP}(\text{INDEX}(\text{LINEST}(\text{LN}(\text{height1}:\text{heightN}), \text{LN}(\text{volume1}:\text{volumeN}), , , 1, 2))$$

$$b = \text{@INDEX}(\text{LINEST}(\text{LN}(\text{height1}:\text{heightN}), \text{LN}(\text{volume1}:\text{volumeN}), , , 1)$$

At this point a very sensible question is how the above functions will be applied in the use case of this project when they are based on data going up to a maximum of 422.4 meters whilst the bottom of the sediment bypass tunnel, and hence the height at which we will start to see flow of water through the tunnel within the model, is at 414 meters. The answer is that this volume-height equation cannot account for that. However, it can be manipulated to do so with a very simple change. The flow into the tunnel starts, of course, at 0 m³/s and hence the first few time steps will show an inflow volume of 0 hm³. However, if we assume that the water height is right below 414 m then there is a starting volume within the reservoir and then that volume will be added to the inflowing volume of the tunnel in the first-time step. This in turn forces the water height to be assumed at a higher value, thus projecting a value closer to that behind the weir which in turn is the one that should be given as an input to the tunnel flow model.

It must be noted here that whilst the volume-height equation is of the reservoir, the water heights shown and used within the tunnel flow model are not those of the main dam reservoir but instead of the weir only. Water overflows the weir and properly enters the reservoir but the water height within the reservoir will assume heights equivalent to the actual volume of water within the reservoir itself which is by no means the artificial and very high starting volume which results from the

high starting water height that was previously set so as to facilitate the aforementioned process.

Due to the method explained in the previous paragraph, it should also be apparent that we expect to see quite high height values from the volume-height equation. Thus, to receive more accurate results from that equation it is useful to calculate a and b based on higher heights and volumes from the previously shown height and volume table. In particular, the starting height of the array chosen in this project for a and b was 411.2 meters which is equivalent to 23.73 hm³ of reservoir volume. For generalisation purposes, three sets of a and b values were created: a1-b1, a2-b2 and a_{low}-b_{low}. a1-b1 starts at 383 meters of height and ends at 409.6, a2-b2 starts at 411.2 m and ends at 422.4 m and a_{low}-b_{low} starts at 383 m and ends at 385.6 m. That said, a1-b1 and a_{low}-b_{low}, whilst added as exceptions to the volume-height equation in the tunnel flow code, are generally not used as they represent water volumes far below the starting one. Specifically, the volume limits in hm³ for switching between the low, 1st and 2nd set of a-b as well as the values of a and b in each set and the maximum water height calculated based on the water inflows and also the opposites of all those values for finding volume from water height, which was used to find the set starting volume from the set starting water height, are shown in the table below:

Table 14: Volume-Height(Find z from V) parameters and their opposites, Height-Volume parameters(Find V from z)

zmax(m)	424.905	Opposite(Find V from z)
a _{low}	384.48	6.84E-260
b _{low}	0.010	100.26
a1	382.97	1.95E-127
b1	0.020	49.06
a2	376.63	1.63E-91
b2	0.028	35.25
limit12(hm ³ /opposite: m)	20	408.5
limitlow1(hm ³ /opposite: m)	1.3	385.2

6.3 Constant Parameters of the Tunnel Flow Model

Before we can start developing the tunnel flow model, some parameters must first be set. First, we need to decide on the shape of the tunnel. To simplify the calculations the tunnel has been assumed to be orthogonal in shape. In reality the

tunnel will have more of an egg-like shape or will be orthogonal with an arch on top[22]. The calculations in this project, whilst assuming a perfectly orthogonal tunnel, would not differ at all for an orthogonal tunnel with an arch on top due to the fact that the water is free flowing and thus never reaches the tunnel ceiling where the arch is. The difference between the calculations of this model with a tunnel that is egg-shaped may or may not be significant depending on the maximum horizontal width of the tunnel. Therefore, the real tunnel assumed here is an orthogonal one with an arched ceiling.

Then the width and height of the tunnel must be set. The width has been set at 4.5 meters. The height has been set at 10.5 meters. It must be noted that the height is significant here but the overall surface area of the tunnel opening is reasonable at 47.25 m² which would be slightly lower than the opening of the sediment bypass tunnel of the Nunobiki dam at 49.02 m²[23].

Moreover, a 10.5-meter-high tunnel assumes the extreme scenario of a full diversion of the 100-year rainfall input which is obviously unreasonable. A percentage only of the incoming rainfall would be diverted together with its sediment and that is determined by the systems at the weir that drive water into the sediment bypass tunnel, but there is no way for this model to predict that percentage without further data for the functionality of the weir. Besides, this model predicts the bed load and material loss accurately only if a full diversion is assumed.

Now, the reason behind the necessity of making all calculations based on the assumption of a full diversion of the rainfall water volume by the tunnel has to do with the tunnel flow model itself. Basically, in order to review the full extent of the potential amount of damage incurred by the tunnel during the bypassing of the incoming rainfall event and its sediment, it is necessary for the model to assume that all of the water volume of that rainfall is being bypassed. That is because the calculations for the flow of sediment within the bed load, which in turn is what damages the tunnel, have been made with inputs from the tunnel flow model. For example, the friction velocity requires the hydraulic radius calculated in the tunnel as an input. Hence, if the model considered the realistic scenario where only part of the rainfall water is bypassed then that means that the amount of inflowing sediment would be under-evaluated by the model because the amount of

sediment is tied to the water inflows into the tunnel and thus less water bypassed causes the model to think that less sediment has been bypassed also which is obviously not the case. And since the end result of this model is to estimate the cost of the damages incurred by the sediment bypass tunnel during its annual operation, it is reasonable to endeavour for the calculation of the worst-in terms of damages-case-scenario where all of the water, and hence all of the sediment also, is bypassed.

The problem here is that since the model must assume that all of the rainfall water is bypassed and since the entrance of the sediment bypass tunnel is assumed to have its bottom at the basin level, that naturally causes the water height to quickly rise dramatically and well above the height of the tunnel, if that was set to a more reasonable 7 or 8 meters. The issue with the water level being seen by the model as above the ceiling of the tunnel is that the model immediately turns from a free-flowing surface one to a pressurized one at least for some of the distance of the tunnel. Simply put that is not at all realistic. It greatly increases the damages incurred within the tunnel and as stated before not all of the water gets diverted which means that the real water height within the tunnel would not be as high as shown in the model and hence accepting that the water flow would be pressurized would lead to results that would be wholly unrealistic.

Besides, sediment bypass tunnels are usually not comprised of a tunnel formed in a straight line from start to finish. At the entrance they usually have a steep incline which further aids to the existence of a free flow within the rest of the tunnel but that is difficult to show in a calculation model. Therefore, the usage of a high enough tunnel height allows for the usage of this model as is and relatively accurately shows the effects of the bypassed sediment onto the tunnel itself. Afterwards and with more data present, specifically in regards to the percentage of water that actually gets diverted in such an event, the height of the tunnel can be set to more reasonable levels. At a design stage that would probably require a real-life downscaled model of the tunnel and weir system on which testing can be conducted. However, such a measure is expensive and thus impossible to execute for this project specifically.

Next the length of the tunnel must be determined. In the tunnel flow model that has been set to 4600 meters or 4.6 km. That is the distance in a straight line from

the entrance to the exit of the tunnel. More specifically, the tunnel entrance will be within the reservoir curve that is directly east of the village of Pteria and the tunnel exit will be directly downstream of the dam and at the level of the river basin. It should be noted here that whilst this distance can theoretically be covered in a tunnel constructed in a straight line from its entrance to its exit, in practice the geological circumstances of the interlaying ground might force the pathway of the tunnel to be altered slightly. Any such alterations will obviously lead to a slightly longer tunnel.

At this point we must also determine the exit height of the tunnel. That is much more straightforward than the entrance height. The exit height must be at the height of the river basin directly downstream from the dam. The height of the river basin directly downstream from the dam is nearly the same with the height of the dam's tailwater and the Ladonas dam tailwater is at a height of 372 meters. Therefore, the exit of the sediment bypass tunnel will also be at 372 meters.

With the entrance and exit heights as well as the tunnel length set, the slope of the main part of the tunnel, J_0 , can be calculated and it is 0.0091 or 0.91%. That is slightly less than the tunnel slope of the sediment bypass tunnel of the Miwa dam (1%) in Japan and also it is a slope comparable to those of the tunnels of the dams Nunobiki (1.3%) in Japan and Runcahez (1.4%) in Switzerland [23,2].

Next, we need to set the n-factor. For n_0 that is simply the standard 0.015. For n and under perfect circumstances, n has to change depending on the percentage of the water height to the total height of the tunnel. However, when calculating the height step by step to simulate the flow during a rainfall event, finding n based on what was just mentioned, thus based on y/D , is slightly more difficult. The problem is that a recursive calculation would be necessary in every single calculation step and whilst that's most certainly feasible, that would require significant computing power to handle the sheer amount of data that must be re-evaluated on every step for a variable n to be used. To avoid this issue, a constant n has to be applied instead. Since the local hydraulic losses in the tunnel entrance- which are also the only local hydraulic losses in this system-are calculated separately, an n equal to 0.013 was used.

An unused computational parameter is the water depth at the tunnel exit, y_{exit} . That value is used to find the limitation distance L_{lim} in the case of a pressurized

flow. However, since it was decided previously that the tunnel shall operate under free-flow conditions exclusively, the value set for this parameter is irrelevant.

Then the kinematic viscosity ν is set at the standard value of 0.0000011 and a , the parameter that influences hydraulic height due to the speed of flow, is assumed to be 1. The parameter K for the local hydraulic losses upon entry into the tunnel is set to 0.5. With these parameters out of the way the development of the tunnel flow model can actually commence.

6.4 Main Tunnel Flow Model

The first column of the model is the time which is noted in 30-minute increments. The second column represents the inflows in m^3/s as those were found previously using the HEC-HMS basin model. Then the third column is the inflowing volume of water in hm^3 which is simply the inflow times the time difference of the current and the previous step, or, since the time step is set to be constant in this model, the inflow times the time step. Then the fourth column calculates S in hm^3 . Now S is the total functional volume, which means the volume not yet passed through the tunnel in the previous step plus the new volume that has arrived due to the rainfall in the same step. In the first step, S is equal to the set starting volume plus the incoming rainfall volume but since the rainfall volume in the first step is zero, it is equal to the set starting volume only.

The fifth column calculates the water height based on the height-volume equation parameters a and b which were detailed previously. The sixth column denotes the water depth from the bottom of the tunnel. Both the water height and the depth are specifically noted for the water at the entrance of the tunnel as both change through the flow of the water within the tunnel. The water depth specifically changes until it reaches the stable depth value, y_0 . That is due to the kind of water slope that is constantly present due to the specific design choices made already and that slope is S_2 .

The seventh column, L_{lim} , denotes the distance of pressured/limited flow within the tunnel. However, since the design here is of an exclusively free-flow tunnel, L_{lim} is always 0. The eighth column denotes the surface area covered by water which is simply the width of the tunnel times the depth of the water since the

tunnel is orthogonal. The ninth column is the water perimeter which is the width of the tunnel plus two times the water depth. The tenth column is the hydraulic radius which is the ratio of the water surface area divided by the water perimeter.

The eleventh column is the water slope in case of pressurized flow and is thus unused in this model.

The twelfth column calculates the speed of the water flow at the entrance. The Manning equation was used for this purpose and that equation is as follows:

$V = \frac{1}{n} R_h^{2/3} J_o^{1/2}$	eq. 14 [24]
---------------------------------------	--------------------------------

J_0 denotes the slope of the stable flow which is parallel and hence equal to that of the tunnel and that was what was used for eq. 14. It must be noted here that this is not entirely accurate. The water flow takes some time to reach the stable depth within the tunnel. In fact, it can be argued that it might not reach the stable depth at all. However, looking at the difference between y and y_0 in the model, that is small enough to make it really improbable that the stable depth is not reached at all. In the vast majority of the time steps the stable depth is reached extremely quickly simply due to the small difference between y and y_0 and in the rest of the steps, or, in other words, during the peak of the rainfall, it is reached but in the middle of the tunnel.

The only way to know the above for sure is by re-doing the entire process with an integrated Standard Step Method process which will make calculations per distance increment for every time step. The problem then becomes the same as with the usage of a variable n . The number of calculations and repetitions in those calculations required to have an SSM procedure embedded into the model cannot be handled by the computing system currently available to me. Most likely this can be resolved by constructing the entire tunnel flow model on matlab or python and then extracting the required results into an excel sheet but the creation of such a program is beyond the scope of this project as it would require a project possibly as lengthy as the current one. Besides, since the water always reaches the stable depth in this project based on what was mentioned previously, the speed calculated above is definitely achieved at some point within the tunnel and in fact is the speed that is present for the vast majority of the water flow within the tunnel.

The thirteenth column calculates the Reynolds number as the water speed times the tunnel width divided by the kinematic viscosity ν . The fourteenth column calculates the outflow from the tunnel in m^3/s as the water speed times the water surface area. The flow is constant per time step throughout the tunnel, but the speed and surface area are not. The surface area decreases further along the tunnel until it reaches the stable water depth and consequently the water speed rises until that point is reached.

The fifteenth column is the last column directly used for the tunnel flow model and it calculates the amount of water that exits the tunnel in that particular step in hm^3 as the outflow found in the fourteenth column times the time step. Note that there might water flow even before the rainfall event. That is both due to the structure of the model itself but also because the sediment bypass tunnel will never automatically be opened precisely when the rainfall water of that rainfall event begins to arrive. It will be already open for possibly hours before that in anticipation for the rainfall event and can potentially be diverting water even before the rainfall event.

The effectiveness of the handling of the bypass tunnel plays a significant role here as good handling lowers the amount of water lost through the tunnel by opening the tunnel at just the right time for just the sediment-carrying rainfall water to be diverted. Worse handling will lead to more water being lost without actually raising the amount of sediment diverted. The fact that the entrance of this tunnel is relatively close to the entrance of the reservoir acts as a failsafe for this matter also. That is because even if the tunnel is left open for more time than absolutely necessary it will still divert no water until there is a sediment-carrying rainfall event to raise the water levels enough for water and sediment to enter the tunnel.

Moving on, the columns till the one calculating Q_{final} are designed to show the free-flowing portion of the tunnel in case the flow started out as pressurised. However, since it was decided that the tunnel should be fully free-flowing, these columns remain unused in this project. Then, Q_{final} and V_{out} show the final outflow from the tunnel in m^3/s and the final volume of that outflow in hm^3 . Since there is only one flow section in this model those values are equal to those found in columns fourteen and fifteen respectively. Last but not least the V_2 columns calculates how much water is still within the reservoir after V_{out} is

deducted from the initial volume S. V2 is then added onto the S of the next step and the model continues with the same steps described previously.

Overall, the flow out of the tunnel as well as the tunnel’s retention of the incoming rainfall flow in relation to time as well as the water height at that same time are shown in the following diagram:

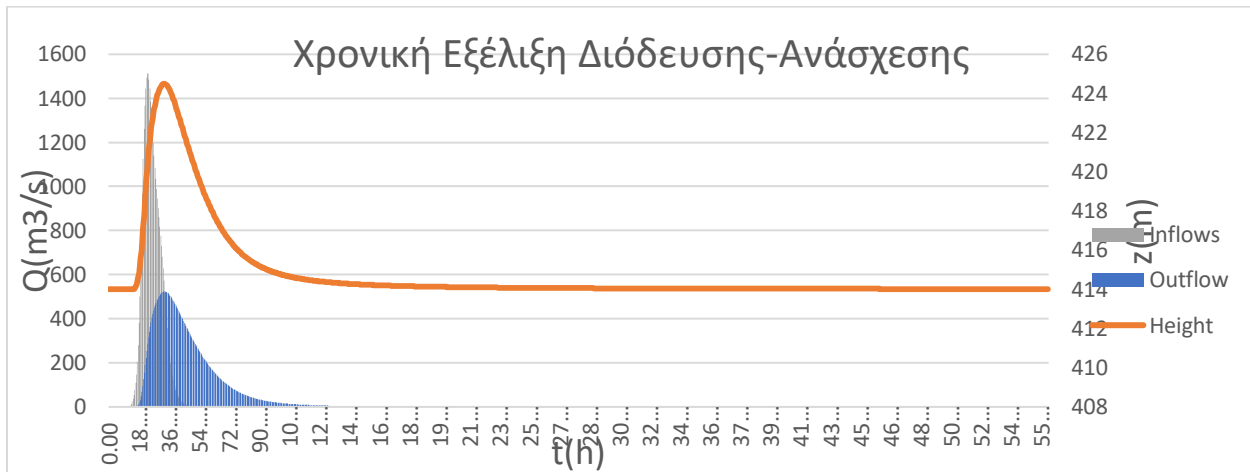


Figure 15: Throughflow-Retention time diagram with water height

6.5 Additional processes

In addition to the process described before some columns were added to the left of the model to check for the slope kind. The slope kind must be steep in order for a sediment bypass tunnel to function properly. To check for that the stable depth, y_0 , was found based on the following equation:

$y = \frac{1}{b} \left[\frac{Qn}{J_o^{1/2}} (b + 2y)^{2/3} \right]^{3/5}$	eq. 15 [24,2]
--	----------------------------------

Eq. 15 is an equation that works by repetition. To make this work the following VBA code was added to the excel sheet of the tunnel model:

```

Function STDEP(b, Q, n, J0, initvalue, target)
    Value = (1 / b) * (((Q * n) / (J0 ^ 0.5)) * ((b + initvalue) ^ (2 / 3))) ^ (3 / 5)
    oldvalue = Value
    Do
        Value = (1 / b) * (((Q * n) / (J0 ^ 0.5)) * ((b + oldvalue) ^ (2 / 3))) ^ (3 / 5)
        Count = Abs(Value - oldvalue)
        If Count <= target Then
            Exit Do
        Else
            oldvalue = Value
            Value = (1 / b) * (((Q * n) / (J0 ^ 0.5)) * ((b + oldvalue) ^ (2 / 3))) ^ (3 / 5)
            Count = Abs(Value - oldvalue)
        End If
    Loop
    STDEP = Value
End Function

```

Figure 16: VBA loop code for the calculation of the stable water depth y_0

Wherever a comparison with the stable depth was stated within this model, it refers to the stable depth found with the above code per time step.

Then the critical depth, y_c , was found as per the following equation:

$y_c = \left(\frac{Q^2}{b^2 g} \right)^{1/3} = \left(\frac{q^2}{g} \right)^{1/3}$	eq. 16 [24,3]
---	----------------------------------

Then the two depths were compared between each other and with the depth found in the tunnel flow model. Based on that information, if $y_0 < y_c$, then the slope is steep, else, if $y_0 > y_c$, then the slope is mild. If the slope is steep then if $y < y_0$ the slope kind is S3, if y is between y_c and y_0 then the slope is S2 and if y is over y_c then the slope is S1. If the slope is mild then if $y < y_c$ the slope kind is M3, if y is between y_0 and y_c then the slope is M2 and if y is over y_0 then the slope is M1 [\[24,4\]](#). The column next to the one calculating y_c is the one that makes this consideration and as seen there the slope kind, whenever there is flow of water through the tunnel, is always an S2 meaning that the water slope is steep and the water depth is lower than the critical depth but higher than y_0 and slowly converges towards y_0 , which in turn is the expected slope kind in a sediment bypass tunnel.

Another additional item is the following table which shows the total amount of water diverted during all time steps, the minimum and maximum outflow from the tunnel and the minimum and maximum amount of the outgoing water volume.

Table 15: Final outflow in m³/s, volume outflow and total amount of volume outflow in hm³ from tunnel

	TotalVout(hm ³)
	66.43
minQfinal(m ³ /s)	minVout(hm ³)
0.149	2.68E-04
maxQfinal(m ³ /s)	maxVout(hm ³)
523.46	0.94

The total incoming rainfall volume as well as the percentage of that that is calculated to have been diverted in the model, the bed load percentage that this model leads to, the maximum water depth reached in the model-which is not the actual maximum water depth that would have been reached in such an event within the tunnel but it is the number used to determine the computational height of the tunnel in this model-and the annual damage incurred by the tunnel annually based on its characteristics are shown in the following table:

Table 16: Overall results table for flow through the sediment bypass tunnel

Itotal(hm ³)	TotalOut(%)	Bed Load(%)	y,max(m)	Annual Damage(Euros)
66.77	99.50%	16.10%	10.49	€ 117,632

The calculation of the bed load and of the annual damage are shown as a summary in this table but their calculation will be explained in detail in the next chapter.

Chapter 7 - Calculation of Tunnel Material Loss due to Sediment Flow

There are several models that calculate the material loss of sediment bypass tunnels. The one used in this project is the Ishibashi model of 1983. However, just to get to the calculations of that model other data are first required. Instead of going directly to the Ishibashi model and then going back to explain how that data was found, the step-by-step process followed within this project will instead be shown, which culminates in the calculations of the Ishibashi model.

7.1 Constant Parameters

First of all, some basic parameters are necessary. These are constant as they do not change regardless of the time step and thus have been noted separately in the following table:

Table 17: Constant parameters for the calculation of the abrasion in the sediment bypass tunnel

ρ_s (t/m ³)	n for q_s^*	β (auxiliary parameter)(m/N ^{2/3})
1.6		1.5
Volume of one grain(by approximation of a sphere)(m ³)	τ_c^* based on the Shields equation(in relation to θ_c^*)	M_p^* (submerged particle weight in kg)
0.00022	0.00072	0.13
Average Grain Diameter in bed load(mm)	Average Grain Diameter in bed load(m)	D^* (dimensionless grain size)
75	0.075	226506
	ρ_{steel} (t/m ³)	Critical Shields Number(θ_c^*)
	7.85	0.00065
μ_s (Dynamic Friction coefficient)	M_p (particle mass)	
0.3	0.35	
	λ_p (air porosity)	
	0.4	
ρ_w (t/m ³)	n_i	
0.1	2716.24	
s	n_1 (sediment gravel over concrete)(N/m ²)	
16	23634870000	

ρ_s in t/m³ is the average density of the sediment, the same one that had been set in chapter 4. ρ_{steel} in t/m³ is the average density of steel which is 7.85 t/m³ and ρ_w is the density of water which is 0.1 t/m³.

n for q_s^* is a parameter in the calculation of q_s^* , the dimensionless dry sediment weight per unit channel width, based on a generalized derivative of the original

Meyer-Peter Mueller formula(1948) for bed load sediment transport. This n is always equal to 1.5 as also shown in the above table[26].

The average grain diameter in the bed load, D50, is the one that both the Ishibashi and Auel models work with and that is 7.5 cm or 75 mm[27], as noted in the table above also. Of course, it is preferable for the model to be run separately for the various different grain sizes present in the sediment flow of a dam’s subbasin but the required granulometry of the bed load sediment of the Ladonas reservoir has not been conducted and hence this cannot be done.

The volume of one sediment grain is calculated by approximation as equal to that of a sphere with a diameter equal to the average grain diameter.

The rest of these constant parameters are directly required for the Ishibashi abrasion model[27,2]:

The auxiliary parameter β is in $m/(kgf)^{(2/3)}$ and calculated as follows:

$\beta = \left[2.5n_1^{2/3} (D/2)^{1/3} \right]^{-1}$	eq. 17
--	--------

In eq. 17 D is the average grain diameter noted before and n1 is another auxiliary parameter which has a constant value of $2.41 \cdot 10^9$ kgf/m² in the Ishibashi model and this was what was used in this project also, thus yielding β equal to $1.45 \cdot 10^{-7}$. More generally n1 is calculated as follows:

$n_1 = \frac{4}{3(k_1 + k_2)}$	eq. 18
--------------------------------	--------

In eq. 18 k1 and k2 are auxiliary parameters that account for the Young’s modulus and Poisson’s ratio of both the particle and invert materials. Still, since this project uses the Ishibashi model, the previous constant value of n1 has been used. n1 itself is noted in the constants table also but after being converted into N/m² via multiplication of its constant value $2.41 \cdot 10^9$ kgf/m² with 9.807.

The particle mass, Mp, in kg, is calculated as follows:

$M_p = 1/6\pi\rho_s D^3$	eq. 19
--------------------------	--------

In eq. 19 ρ_s in t/m³ is the average density of the sediment noted previously and D is the average grain diameter that was also noted previously. Based on these same

parameters the submerged particle weight in kg was also found based on the following equation:

$M_p^* = 1/6\pi(\rho_s - 1000)D^3$	eq. 20
------------------------------------	--------

Next the dimensionless average grain diameter D^* is calculated based on the average grain diameter D as follows:

$D^* = [(s-1)gD^3]^{0.5}/\nu$	eq. 21
-------------------------------	--------

In eq. 21 ν is the kinematic viscosity which was set in the tunnel flow model of chapter 6 and s is the ratio of the average sediment density, ρ_s divided by the water density, ρ_w . Based on the previously stated values for ρ_s and ρ_w , s equals 16 in this project and that is also noted in the constants table presented in the beginning of this chapter.

Then based on the dimensionless average grain diameter the critical shields number θ_c was found based on the following equation:

$\theta_c = 0.0907D_*^{-2/5}$	eq. 22
-------------------------------	--------

Eq. 22 was developed by Ishibashi(1983) based on Novak and Nalluri(1975).

The dimensionless critical shear stress, τ_c^* , is 0.047 as per the Meyer-Peter Mueller transport formula[25]. However, that value of τ_c^* is meant for the usage of the Meyer-Peter Mueller transport formula with a flow at a stage number of 8. That is simply not the case in this project where the stage number fluctuates and can assume values both higher and lower than 8. Besides, the generalized version of the Meyer-Peter Mueller transport formula[26,4] can be used with different τ_c^* values.

In this project the important part is that the critical dimensionless Shields number, θ_c^* , and critical dimensionless shear stress, τ_c^* , must correlate as they both refer to the values of the dimensionless Shields number and dimensionless shear stress respectively that occur when sediment begins to move. Since both θ_c^* and τ_c^* are used for the same flow model, they must also show the same moment that the sediment begins to move for their respective non-critical values and hence they must correlate. This correlation is easily found via the Shields formula which gives the Shields parameter as follows:

$$\theta = \frac{\tau}{(\rho_s - \rho)gD}$$

eq. 23
[31]

In eq. 17 ρ_s is the density of the sediment, ρ is the density of water, D is the average grain diameter, τ is the shear stress and θ is the Shields parameter. By replacing θ_{c^*} for θ and τ_{c^*} for τ and then solving for τ_{c^*} we can find the τ_{c^*} that is equivalent to the θ_{c^*} that was found in the previous step.

The air porosity, λ_p , was set to 0.4 as per the Ishibashi model [27,6]. Then based on that air porosity, λ_p , the average sediment density, ρ_s , and the particle mass, M_p , the amount of particles per unit of volume, n_i , in 1/m³ was found as per the following equation:

$$n_i = \frac{(1 - \lambda_p)\rho_s}{M_p}$$

eq. 24
[27,7]

The last constant parameter is μ_s , the static dynamic friction coefficient, which has been set to 0.3 as per the Ishibashi model.

This concludes the calculations for the stable parameters of the process that will be explained in the rest of this chapter. It must be noted here that much like with several of the equations already stated in this chapter, like the equation for θ_{c^*} , there are several equations and processes that can calculate many of the values that will follow. Those values that can be calculated in many ways are usually the result of experimental procedures which tend to have differing inputs and hence different results. The equations chosen in this project were either those coming from projects with inputs matching those of this project, e.g. in regards to the average grain size or stage number, or were noted under the Ishibashi model in which case they were preferred over other alternatives to maintain consistency with the main model being used in this part of this project.

[7.2 Calculation of the bed load sediment volume](#)

Before anything else, it should be mentioned that two columns are noted within the excel sheet of this project for each one of the values that will be calculated

next. That was meant to account for the possibility of a split flow, or in other words a flow that would start as pressurized and then turn into a free flow. However, and as mentioned many times already, this model operates under the design decision that the flow within the tunnel is always a free flow and never pressurized. Thus, the second column for all of the following values is left unused.

At any rate, the first value that must be calculated is the friction velocity U^* in m/s. The calculation of that is simply $(g \cdot R_h \cdot S)^{0.5}$, where R_h is the hydraulic radius from the tunnel flow model and S is the slope of the tunnel. Technically speaking S should be the energy slope but, for the same reasons stated in regards to the water speed in chapter 6, the slope of the tunnel is used.

Then the Shields parameter θ is calculated based on the friction velocity U^* , the average grain diameter D and the density ratio s as follows:

$\theta = U^2 / [(s-1)gD]$	eq. 25 [27,3]
----------------------------	----------------------------------

The stage number was found as per Sklar and Dietrich(2004)[\[28\]](#). Thus, the ratio of the Shields parameter divided by the critical Shields parameter is first calculated and then that ratio minus one equals the stage number. Wherever that ratio was less than 0, it was set to 0. The stage number denotes the “stage” of the flow. Generally, the higher the flow, the higher the stage number. If the stage number is zero then that means that there is not a high enough flow of water for there to be sediment transport.

Next the ratio of the sediment saltation length, L_p , to the average sediment diameter, D , was found based on the Shields parameter and the critical Shields parameter as per Ishibashi(1983) in turn based on Ishibashi and Isobe(1968):

$\frac{L_p}{D} = 100(\theta - \theta_c)^{1.21}$	eq. 26 [27,4]
---	----------------------------------

Whenever the Shields parameter was less than the critical Shields parameter this calculation would result in an error and was set to zero. This essentially means that those time steps do not have a water flow high enough, or, in other words, with a high enough stage number, to have saltating sediment. That is to be expected since, if L_p/D equals zero, then L_p , the saltation distance, will also be zero and hence there is no saltation. That said the steps with L_p/D equal to zero

actually have no sediment transport at all which is evident from the fact that they align with all the steps where the stage number equals zero.

Then the shear stress τ was calculated as the result of $\rho_w * g * y * S$ where ρ_w is the water density, y is the water depth from the tunnel flow model and S is the tunnel slope or stable depth slope for the reasons noted in chapter 6.

The non-dimensionalization of the shear stress, τ^* , was done based on the equation used by the Meyer-Peter Mueller sediment transport formula which is the following one:

$\tau^* = \frac{\tau}{(\rho_s - \rho)(g)(D)}$	eq. 27 [25,2]
---	----------------------------------

In eq. 26 ρ_s is the sediment density, ρ is the water density and D is the average grain diameter with the input being τ , the shear stress, as that was found previously. A small check has been added over the column calculating the dimensionless shear stress τ^* that checks if at least the maximum dimensionless shear stress is over the value set previously in the constants table for the dimensionless critical shear stress, τ_c^* . And indeed, the maximum value is above that critical value as seen in that table which is also shown below:

Table 18: Maximum dimensionless shear stress and check of whether it is above the critical dimensionless shear stress

>Critical Shear Stress?	TRUE
Max Non-dimensional shear stress, $\tau^* 1$	0.09

The generalized version of the Meyer-Peter Mueller sediment transport formula uses the parameter as in the calculation of the dimensionless dry sediment weight per unit channel width. as is calculated as follows:

$\alpha_s = 1.6 \ln(\tau^*) + 9.8 \approx 9.64\tau^{*0.166}$	eq. 28 [26,2]
--	----------------------------------

In eq. 28 τ^* is the dimensionless shear stress calculated just before.

Moving on, q_s^* , the dimensionless dry sediment volumetric discharge per unit channel width, is calculated based on the generalized version of the Meyer-Peter Mueller sediment transport formula which is as follows:

$q_s^* = \alpha_s (\tau^* - \tau_c^*)^n$	eq. 29 [26,3]
--	----------------------------------

Where in eq. 29 q_s^* is the parameter calculated in the previous step and τ^* is the dimensionless shear stress calculated before and τ_c^* is the critical dimensionless shear stress which was set in the constant parameters table at the start of this chapter. Whenever the dimensionless shear stress is below the critical one in which case eq. 29 results in an error, q_s^* was set to be zero, meaning that the water flow was too small for there to be sediment transport.

The dry sediment volumetric discharge per unit channel width, q_s , is then calculated by using Hans Einstein's nondimensionalization equation for q_s but in reverse. Hans Einstein's nondimensionalization of q_s is as follows:

$q_s^* = \frac{q_s}{D \sqrt{\frac{\rho_s - \rho}{\rho} g D}}$	eq. 30 [25,3]
---	----------------------------------

As already mentioned, to find q_s based on q_s^* eq. 30 is used in reverse. Also, in eq. 30 D is the average grain size, ρ_s is the density of the sediment and ρ is ρ_w , the density of the water.

Knowing q_s from the previous step, the bed load sediment flow in m^3/s is simply q_s times the width of the sediment bypass tunnel. In turn, V_{ts} in hm^3 , the sediment volume in the bed load, is easily found by multiplying the sediment flow of the bed load with the time step, or-more generally speaking for cases where the time step is not constant-the difference of the time between the current and the previous step. By summing up the V_{ts} of all time steps we find the total amount of diverted bed-load-sediment by the sediment bypass tunnel during the diversion of the sediment produced by this rainfall event.

That total event V_{ts} is then translated to a total daily V_{ts} via simple analogy based on the total sediment diversion time. In other words, the total daily V_{ts} is equal to the total event V_{ts} multiplied by the ratio of 24 hours to the time length of all time-steps for which V_{ts} was counted as anything above zero. That time length has been found to be 216.5 hours in this project. That daily V_{ts} , or, more precisely, V_{ts} per day of this event, is then converted into the V_{ts} of an average day via multiplication with the ratio of the total rainfall of the average erosive rainfall event divided by the total rainfall of this 100-year rainfall event. This ratio was also

mentioned in more detail in chapter 6. Now, the Vts of an average day is then multiplied by the number of erosion days per year which was a value presented in chapter 4. This multiplication results in the average Vts per year in hm³.

Then, the bed load percentage is usually given from data in measurements of weight and so Vts per year in hm³ was multiplied by ps, the density of the sediment, giving us that same result in tons instead of hm³. That number is about 26443 tons of bed-load-sediment diverted per year. Then the average yearly sedimentation calculated based on the R.U.S.L.E. model in chapter 5 was also converted to tons per year in the same manner and the result was 164212 tons of average total sediment diverted per year. The ratio of the yearly tons of total sediment to the yearly tons of bed-load-sediment is the bed load percentage which, based on the numbers calculated previously, equals 16.10%. A bed load percentage of 16.10% is a somewhat high but reasonable number. As a comparison, the sediment bypass tunnel of the Mud Mountain dam has a bed load percentage of 11%[\[6,3\]](#).

7.3 Calculation of the tunnel abrasion/material loss

The next steps are entirely from the process of the Ishibashi model(1983)[\[27,5\]](#):

Lp is the saltation length in meters found by multiplying the previously calculated Lp/D with D, the average grain size.

Ni denotes the impact frequency which means how often saltating sediment hit the tunnel floor. That value is simply the length of the tunnel set in chapter 6 divided by the saltation length Lp.

The impact force of that saltating sediment Fi is calculated based on the submerged particle weight Mp*, the Shields parameter θ and the critical Shields parameter θc as follows:

$F_i = 1.95 \times 10^3 M_p^* (\theta - \theta_c)$	eq. 31
--	--------

Note that eq. 31 results in an Fi in kgf. To translate that into N simply multiply by 9.807.

This impact force F_i is combined with the auxiliary parameter β to result in the single impact energy of the saltating sediment E_i which is calculated as follows:

$E_i = \beta F_i^{5/3}$	eq. 32
-------------------------	--------

Then we calculate the result of the following multiplication: $E_i \cdot N_i \cdot n_i$. Here E_i is the single impact energy in Nm that we just calculated, N_i is the impact frequency found two steps before and n_i is the amount of particles per unit of volume which was set in the constants table at the start of this chapter.

Next, we need to find the particle impact angle γ_{im} which is found by approximation based on the Shields parameter and the critical Shields parameter:

$\gamma_{im} \approx \frac{U_p}{V_s} = 19.2(\theta - \theta_c)^{-0.13}$	eq. 33
---	--------

And now we calculate the following multiplication: $\gamma_{im} \cdot E_i \cdot N_i \cdot n_i$, where γ_{im} is the particle impact angle we just found, E_i is the single impact energy in Nm calculated previously, N_i is the impact frequency found a few steps before and n_i is the number of particles per unit of volume which was set in the constants table at the start of this chapter.

Now the two multiplications made must be summed across all time steps. That is because the total kinetic energy E_k and the total friction work W_f are calculated based on the following eq. 34 and eq. 35 respectively:

$E_k = 1.5V_{ts} \sum E_i N_i n_i$	eq. 34
------------------------------------	--------

$W_f = 5.513\mu_s V_{ts} \sum \gamma_{im} E_i N_i n_i$	eq. 35
--	--------

For eq. 34 we take the sum of all $E_i \cdot N_i \cdot n_i$ and multiply it by 1.5 times the total event V_{ts} . For eq. 35 we take the sum of all $\gamma_{im} \cdot E_i \cdot N_i \cdot n_i$ and multiply it by 5.513 times the total event V_{ts} times the dynamic friction coefficient μ_s which had been set in the constants table at the beginning of this chapter.

Following the previous calculations, we now need to set the material property constants $C1$ and $C2$ for concrete and steel in m^2/kgf and then turn them into m^2/N by dividing with 9.807. The material constants used in this project are the

ones proposed by the Ishibashi model and specifically they come from the following table:

Table 19: C1 and C2 Ishibashi model material parameters for concrete and various types of steel

Material	C ₁ [m ² /(kgf)]	C ₂ [m ² /(kgf)]
Concrete	1.189×10 ⁻⁷	1.135×10 ⁻⁸
Steel (SM 41)	3.73×10 ⁻¹¹	6.59×10 ⁻¹¹
Steel (HT 80)	2.53×10 ⁻¹¹	4.78×10 ⁻¹¹
Steel (SUS 304)	2.04×10 ⁻¹¹	3.25×10 ⁻¹¹
Steel (SCMnH 11)	1.18×10 ⁻¹¹	1.33×10 ⁻¹¹

For concrete, C1 and C2 are set as per the only entry set in the table. The consideration for the C1 and C2 of steel is simply the worst-case scenario or in other words the C1 and C2 of the steel category of SM 41. That is because the kind of steel that will be used in the construction of the tunnel will be determined by the necessities for the integrity of the tunnel itself and not so much by its resistance against the abrasion caused by sedimentation. However, this project does not aim to design the tunnel itself as that is plain impossible without adequate knowledge of the underlying geology of the area. Thus, the best that can be done is the assumption of the worst-case scenario as mentioned before.

Finally, we come to the main abrasion equation of the Ishibashi model which uses the total kinetic energy Ek and the total friction work Wf which we have calculated as well as the sets of C1 and C2 that were just set. This equation is as follows:

$V_a = C_1 E_k + C_2 W_f$	eq. 36
---------------------------	--------

Eq. 36 calculates the material loss from the tunnel due to abrasion caused by the sediment being transported in m3. Eq. 36 must be used separately for steel and concrete. This project only adds up the cost of the damages from the two categories, if both concrete and steel are used in the tunnel invert, in the end.

However, it must be noted here that in eq. 36, and as also seen in the calculations, C2*Wf, which represents the grinding stress, is massively higher than C1*Ek. In particular, in this project and for this rainfall event, we measure 1152 m3 due to C1*Ek but 4712 m3 due to C2*Wf for the abrasion of concrete.

The issue with this is that $C2*Wf$ causes the abrasion to be extremely over-estimated without any reasonable basis. That is because concrete by itself is brittle (as per Head and Harr 1970) and thus it is, in reality, barely affected by grinding and thus $C2*Wf$ that represents the damage due to the grinding stresses should be omitted as it is negligible in reality. In fact, many researchers omit the grinding portion of eq. 36 (Sklar and Dietrich 2001, 2004, Auel et al. 2015). Thus, in this project, $C2*Wf$ is shown as calculated previously but it is omitted in the case of concrete.

Having said the above, we must remind ourselves that whilst concrete is brittle, steel is very much ductile. Due to that $C2*Wf$ should not be omitted in the usage of eq. 36 for steel. Thus, the final equations used to find the abrasion volume were $C1*Ek$ for concrete and $C1*Ek+C2*Wf$ for steel. The final results were an abrasion of 1152 m³ for concrete and 28 m³ for steel per this rainfall event. Those values were then converted into per day of event values in the same manner as Vts was converted from event Vts to per day of event Vts . Then those per day of event values were turned into average daily values again in the same manner that the per day of event Vts was converted into an average daily Vts , which was by multiplying the per day of event Vts with the rainfall ratio of the total average rainfall amount to the total 100-year rainfall amount. Then the daily abrasion volume, Va , in m³ was multiplied by the number of erosive rainfall days per year and the final result was a yearly abrasion of 1069 m³ for concrete and 26 m³ for steel.

7.4 Estimation of the annual repair cost of the tunnel

Whilst knowing the yearly abrasion amount is a nice value to have, the real question is how that abrasion translates into cost. For that, one last consideration must be made: what role does steel play in the invert of the tunnel? If steel refers to just the steel bars within the construction, then the “steel abrasion” calculated in the previous paragraph should be ignored because the steel bars are protected deep within the concrete. The only exception to this is the case where the damage dealt to the invert is ignored over multiple years and it also reaches the steel bars at some point. But even that is unlikely.

The case in which the abrasion of steel should absolutely be considered is if steel linings are placed over the concrete structure of the floor to protect the concrete invert. In that case, the abrasion of steel must be fully taken into account but, at the same time, the abrasion damage dealt to the underlying concrete will also be somewhat mitigated.

In this project and to simplify the calculations, the tunnel invert has been considered to be exclusively concrete without steel linings and thus the cost of steel is ignored in the final calculations. That said, the cost of steel is mentioned in the excel procedure for informative purposes, but it is ignored in the final sum for the yearly damage cost.

The next point has to do with how the cost is considered. The type of concrete used in the invert will be the standard one used in tunnel construction which is C25/30(as per Prof. Basileios Marinos). The cost of supply, transportation and gravitational laying of un-reinforced C25/30 concrete is about 110 euros per m³ with VAT included(as per Prof. Emmanuel Vougioukas).

The cost of steel is subject to a lot more fluctuation than concrete and so the cost of the quarter that this project was finished at was used, that being of Q3 2024. The cost was extracted from the data present in the website of “FOCUSECONOMICS” in the section about the prices of steel in Europe. In Q3 2024 that was 657 USD/mt[29]. On the day of writing this passage(6/11/2024), 1 USD equals 0.933144 EUR[30]. That means that 657 USD/mt equals 613.08 EUR/mt. In turn, 1 mt(metric ton) is equal to 1.102311 t(tons). Thus, the price of steel is 556.17 EUR/t in Q3 of 2024 and that was what was used in the calculations of this project. For steel, to convert the abrasion from m³ to t, the abrasion was multiplied by the average density of steel which was mentioned in the constants table at the beginning of this chapter.

After being the steel abrasion converted to tons of yearly abrasion, that number was then multiplied by the price mentioned just before and that resulted in the average yearly damage cost of steel for this project which was € 113,021.

However, because it was decided that no steel linings would be present in the invert of the tunnel, this cost was ignored in the actual average yearly damage cost of the tunnel. The average yearly damage cost of the tunnel was thus equal to, exclusively, the cost of damages of the concrete. To find that cost, the

aforementioned cost of concrete per m³ was multiplied by the amount of abrasion in m³ calculated before. The final result of that calculation, and thus the final average yearly damage cost of the entire tunnel, was € 117,632.

Lastly, a simplistic estimation was given for the overall cost of damages over a period of 10 years by multiplying the previous result by 10. The result of that was € 1,176,315 in average abrasion damages over a period of ten years. It must be emphasized here that the damage costs do not rise in a linear fashion like this calculation might seem to imply. € 1,176,315 would be the cost of damages over a period of ten years if the tunnel is repaired, as it should, every year. If the damages to the tunnel are left unattended then they will rise at a much faster rate every year that they are not repaired. In other words, if the tunnel is not repaired, or not properly repaired, on an annual basis then the damages incurred by year 10 won't be € 1,176,315 but something much higher than that.

All the above considered, a cost of about 118,000 euros in repairs on an annual basis for the sediment bypass tunnel of this project is a significant cost but not something too great in the spectrum of dam repairs. Here it should be clarified that since the cost of the concrete mentioned before includes supply, transportation and gravitational laying as well as VAT, it is roughly equal to the cost of repairs. Of course, the actual repair cost might also contain other secondary costs but those would be quite small in comparison to those already included within the price of the 118,000 euros given before.

Moreover, an annual repair cost of around 118,000 euros is also very much a middle cost in terms of annual sediment bypass tunnel repair costs. As a comparison, the sediment bypass tunnel at the Pfaffensprung dam in Switzerland has an annual maintenance cost of 100,000 CHF which is equal to about 106,476.78 EUR [\[30,2\]](#). The most expensive annual repair costs recorded are from the Asahi dam in Japan which are equal to 200,000 CHF, in turn equal to about 212,947.73 EUR.

Chapter 8 – Conclusions

8.1 Advantages of the process of this project

As can be derived from the manner in which this project has been written this whole procedure is meant as a tool and this text explaining it as a manual on how it should be used. In that context, this project benefits significantly from the fact that it is a complete tool, starting with a very basic input point, that of the rainfall, and going all the way to an end level and usable result, that of the annual repair cost.

The main features of this project that make the aforementioned possible are the splitting of daily rainfalls into steps via the rainfall IDF curve methodology, the detailed calculation of all factors that contribute towards the application of R.U.S.L.E. and the tunnel flow model. In particular, the usage of the rainfall IDF curve methodology for the splitting of standard rainfalls is quite an innovative element within this project.

Moreover, not only does this project have the aforementioned advantages, but it is also flexible enough to be able to operate in the same or similar manner for the inputs of any dam to estimate the annual repair cost of a potential sediment bypass tunnel for their reservoirs.

8.2 Overview of the results for the Ladonas reservoir

The results of this project in regards to the Ladonas reservoir in particular are as follows: sedimentation in the Ladonas reservoir is high and its alleviation via the construction of a sediment bypass tunnel is financially plausible. The calculated sedimentation of the Ladonas reservoir in this project is about 15% and, with a sedimentation rate of about 0.22% per year, that will reach 22% by the 100-year mark of the dam's operational life. Then the annual repair costs of a sediment bypass tunnel in the Ladonas reservoir would measure to about 118,000 EUR, which is doubtless a significant amount but it is by no means excessive for the annual repair costs of a dam project.

A sediment bypass tunnel in the Ladonas reservoir will effectively negate sedimentation within the reservoir thus extending the lifespan of the dam

significantly. This will also remove the need for occasional sediment management measures such as dredging. Additionally, the natural sediment flow downstream of the dam will be restored as if it had never been severed in the first place and any problems of erosion downstream of the dam will be resolved.

As to the matter of water loss, with good handling the sediment bypass tunnel will only work within the confines of erosive rainfalls. This will allow sediment to be diverted whilst minimising the amount of water lost from the reservoir through the sediment bypass tunnel. Still, this point is worthwhile to emphasize: Any pre-cautionary measures taken in the construction of a sediment bypass can be made useless presence of careless handling of the tunnel. A sediment bypass tunnel is a structure with a high construction cost and a high repair cost paid every year throughout its lifetime. And, whilst a sediment bypass tunnel built correctly will not suffer any catastrophic failure, every time it is mismanaged, that will directly translate into a significant financial loss also. But if the management of the tunnel is appropriate then the environmental gain, the preservation of the volume and the extension of the lifespan of the reservoir will greatly outweigh any losses of water during the diversion of sediment.

8.3 Possible future improvements of this project

The entire procedure of this project is, of course, not perfect. Normally the estimation of the sedimentation and of the damages to a sediment bypass tunnel require real life data. Very often, however, such data are not available or are expensive to come by. From the very onset of this project, its aim was to provide a reliable estimation of the damages incurred by a sediment bypass tunnel during its operation especially when such data is absent.

The problem with the lack of such physical information is that some of it is required by this project also and the estimations forced by the lack thereof negatively affect the accuracy of the procedures involved. This mostly has to do with the height at which the entrance of the sediment bypass tunnel is at, which can only be set correctly if the height of the basin has been measured, which is a survey not yet conducted for the Ladonas reservoir. The problem is that without that information the height at the entrance of the tunnel had to be set at 414 m,

based on a less-than-ideal piece of information from google earth, whilst the actual unknown situation might force that height to be completely different, in turn changing not only the elevation that the tunnel entrance stands at but also the slope of the tunnel which is a data-point that massively influences all results regarding the tunnel abrasion.

Furthermore, the fact that the height of the reservoir is not mapped also prevents the creation of a more accurate height-volume equation for the tunnel in particular and forces the usage of the height-volume equation of the reservoir via the assumption of a high starting reservoir volume.

Of course, this project is not without flaws of its own, most notable of which being the tunnel flow model. The model is not incorrect but, as it currently stands, it is not as perfectly accurate as it could be. That is due to the absence of an incorporated SSM procedure. And whilst the addition of that wouldn't influence the results in any major way for reasons explained in chapter 6, it would help in accurately projecting the flow within the tunnel and thus making the model all that much more precise.

Another point that warrants improvement in the tunnel flow model is the lack of consideration for the entrance slope. This slope which exists at the entrance of sediment bypass tunnels helps with the flow of sediment through the rest of the tunnel. However, that slope has not been taken into consideration in the tunnel flow model of this project. That said, introducing that entry slope to the current tunnel flow model is probably the least arduous change to make among all the improvements proposed in this chapter. That is because it simply requires the addition of a flow section before the existing one that will otherwise function precisely like the existing one and will then pass its end flow onto the next section.

Last but not least, and as also mentioned in chapter 4, the limits based on which a rainfall is to be considered erosive should be further studied and modified for the usage of the rainfall IDF curve methodology for small return period rainfalls. The limits used in this project are still arbitrary to a certain extent since they were simply set to whatever values outputted the most sensible results in regards to the R-factor and the number of erosive days per annum. Possibly there might be a correlation between the limits themselves and the time-step that the daily

rainfalls are split into as well as with the total rainfall amount of the rainfall events themselves, but, and as also mentioned in chapter 4, that is definitely worthy of an entirely separate research project of its own and thus beyond the scope of this project.

References

[1] <http://main.hydroscope.gr/> - ΣΧΟΛΗ ΠΟΛΙΤΙΚΩΝ ΜΗΧΑΝΙΚΩΝ - ΤΟΜΕΑΣ ΥΔΑΤΙΚΩΝ ΠΟΡΩΝ & ΠΕΡΙΒΑΛΛΟΝΤΟΣ

[2] <https://csidotinfo.wordpress.com/data/srtm-90m-digital-elevation-database-v4-1/> - CGIAR-CSI - Consortium for Spatial Information

[4,1] [4,2] [4,3] 1η Αναθεώρηση των Σχεδίων Διαχείρισης Κινδύνων Πλημμύρας/ΥΠΕΚΑ-Σχέδια Διαχείρισης Κινδύνων Πλημμύρας-ΟΜΒΡΙΕΣ ΚΑΜΠΥΛΕΣ – 2ος ΚΥΚΛΟΣ, [3] Κουτσογιάννης καί Ξανθόπουλος, 1999

[5] Global rainfall erosivity assessment based on high-temporal resolution rainfall records - Panos Panagos, Pasquale Borrelli, Katrin Meusburger, Bofu Yu, Andreas Klik, Kyoung Jae Lim, Jae E. Yang, Jinren Ni, Chiyuan Miao, Nabansu Chattopadhyay, Seyed Hamidreza Sadeghi, Zeinab Hazbavi, Mohsen Zabihi, Gennady A. Larionov, Sergey F. Krasnov, Andrey V. Gorobets, Yoav Levi, Gunay Erpul, Christian Birkel, Natalia Hoyos, Victoria Naipal, Paulo Tarso S. Oliveira, Carlos A. Bonilla, Mohamed Meddi, Werner Nel, Hassan Al Dashti, Martino Boni, Nazzareno Diodato, Kristof Van Oost, Mark Nearing, Cristiano Ballabio - DOI:10.1038/s41598-017-04282-8 - www.nature.com/scientificreports, page 9

[6] [6,2] [6,3] Abrasion prediction at Mud Mountain sediment bypass tunnel - Auel, Christian; Thene, John; Müller-Hagmann, Michelle; Albayrak, Ismail; Boes, Robert M. – 2017 - <https://doi.org/10.3929/ethz-b-000185304>, page 7

[7] [7,3] Spatio-temporal analysis of rainfall erosivity and erosivity density in Greece - Panos Panagos, Cristiano Ballabio, Pasquale Borrelli, Katrin Meusburger - <http://dx.doi.org/10.1016/j.catena.2015.09.015>, page 163, [7,2] – page 164

[8] Soil Erodibility in Europe - JOINT RESEARCH CENTRE - European Soil Data Centre (ESDAC) - <https://esdac.jrc.ec.europa.eu/themes/soil-erodibility-europe>

[9] Global Hydrologic Soil Groups (HYSOGs250m) for Curve Number-Based Runoff Modeling - <https://doi.org/10.3334/ORNLDAAAC/1566> - https://daac.ornl.gov/cgi-bin/dsviewer.pl?ds_id=1566

[10] Zdruli, P., Jones, R.J.A. and Montanarella, L. Organic Matter in the Soils of Southern Europe. European Soil Bureau Technical Report, EUR 21083 EN , (2004), 16pp. Office for Official Publications of the European Communities, Luxembourg – page 12 -

https://esdac.jrc.ec.europa.eu/ESDB_Archive/eusoils_docs/esb_rr/n15_OMsouth_Europe.pdf

[11]

https://www.fao.org/fishery/static/FAO_Training/FAO_Training/General/x6706e/x6706e09.htm - Chapter 9.2 Soil permeability relates to soil texture and structure – Example Table: Average permeability for different soil textures in cm/hour

[12] A New European Slope Length and Steepness Factor (LS-Factor) for Modeling Soil Erosion by Water - Panos Panagos, Pasquale Borrelli, Katrin Meusburger - Geosciences 2015, 5(2), 117-126; <https://doi.org/10.3390/geosciences5020117>

[13] ΕΘΝΙΚΟ ΜΕΤΣΟΒΙΟ ΠΟΛΥΤΕΧΝΕΙΟ - ΣΧΟΛΗ ΠΟΛΙΤΙΚΩΝ ΜΗΧΑΝΙΚΩΝ ΤΟΜΕΑΣ ΥΔΑΤΙΚΩΝ ΠΟΡΩΝ & ΠΕΡΙΒΑΛΛΟΝΤΟΣ - ΔΙΕΡΕΥΝΗΣΗ ΤΩΝ ΑΠΟΘΕΣΕΩΝ ΦΕΡΤΩΝ ΥΛΙΚΩΝ ΣΕ ΥΔΡΟΗΛΕΚΤΡΙΚΟΥΣ ΤΑΜΙΕΥΤΗΡΕΣ - Διδακτορική Διατριβή - ΔΗΜΗΤΡΗΣ ΖΑΡΡΗΣ - ΑΘΗΝΑ – ΦΕΒΡΟΥΑΡΙΟΣ 2019 – page 66, equation 3.18

[14] Estimating the soil erosion cover-management factor at the European scale - Panos Panagos, Pasquale Borrelli, Katrin Meusburger, Christine Alewell, Emanuele Lugato, Luca Montanarella - <https://doi.org/10.1016/j.landusepol.2015.05.021>

[15] Thanopoulos, R.; Chatzigeorgiou, T.; Argyropoulou, K.; Kostouros, N.-M.; Bebeli, P.J. State of Crop Landraces in Arcadia (Greece) and In-Situ Conservation Potential. Diversity 2021, 13, 558. <https://doi.org/10.3390/d13110558> - page 7, table 2

[16] Support Practices Factor - JOINT RESEARCH CENTRE - European Soil Data Centre (ESDAC) - <https://esdac.jrc.ec.europa.eu/themes/support-practices-factor>

[17] [17,2] Ταμειυτήρες(Διαφάνειες Μαθήματος) - Υδραυλικές Κατασκευές – Φράγματα - 8ο εξάμηνο Σχολής Πολιτικών Μηχανικών - Ανδρέας Ευστρατιάδης & Παναγιώτης Παπανικολάου - Τομέας Υδατικών Πόρων & Περιβάλλοντος, Εθνικό Μετσόβιο Πολυτεχνείο - Ακαδημαϊκό έτος 2021-22 – page 22

[18] <https://www.youtube.com/watch?v=IWxAw6L9UcA> – At the 17:55 mark – The CN table referenced has been made compiled by the creator of this video based on data from NRCS TR-55 and Halley et al. 2000 – ESRI Proceedings

[19] Time of Concentration (TOC) Estimation - By Krest Engineers, LLC - November 29, 2021 – <https://rashms.com/blog/time-of-concentration-toc-estimation/> - Towards the end of the webpage, Figure 19

[20] Υδρολογία πλημμυρών, κάποιες καινοτομίες και η εφαρμογή τους στην πράξη(Διαφάνειες Μαθήματος) - Ολοκληρωμένο Θέμα Υδραυλικού Σχεδιασμού - 9ο εξάμηνο Σχολής Πολιτικών Μηχανικών - Ανδρέας Ευστρατιάδης - Τομέας Υδατικών Πόρων & Περιβάλλοντος, Εθνικό Μετσόβιο Πολυτεχνείο – Νοέμβριος 2023 – page 11

[21] <https://nokyoitsu.com/qscripts/2007/07/excel-trendline-equations.html> - Juan A. Navarro Pérez - Staff Software Engineer at Google, UK

[22] Ismail Albayrak, Romeo Arnold, Dila Demiral, Mohammadreza Maddahi, Robert M. Boes, Field monitoring and modelling of sediment transport, hydraulics and hydroabrasion at Sediment Bypass Tunnels, Journal of Hydro-environment Research, Volume 55, 2024, Pages 1-19, ISSN 1570-6443, <https://doi.org/10.1016/j.jher.2024.05.002> - <https://www.sciencedirect.com/science/article/pii/S1570644324000224> - Chapter 3.1, Figure 1

[23] [23,2] Comprehensive Sediment Management Strategies in Japan: Sediment bypass tunnels - Sumi and S.A. Kantoush - Disaster Prevention Research Institute - Kyoto University - Gokasho, Uji-Shi, 611-0011 – JAPAN - E-mail: sumi.tetsuya.2s@kyoto-u.ac.jp - 34 th IAHR World Congress - Balance and Uncertainty - 33 rd Hydrology & Water Resources Symposium - 10th Hydraulics Conference - 26 June - 1 July 2011, Brisbane, Australia

[24] [24,2] [24,3] [24,4] Παπανικολάου, Π.Ν. (2020). Τυπολόγιο για τους αγωγούς με ελεύθερη επιφάνεια

[25] [25,2] [25,3] Whipple, Kelin (September 2004). "IV. Essentials of Sediment Transport". 12.163/12.463 Surface Processes and Landscape Evolution: Course Notes. MIT OpenCourseWare

[26] [26,2] [26,3] [26,4] Wiberg, Patricia L.; Dungan Smith, J. (1989). "Model for Calculating Bed Load Transport of Sediment". Journal of Hydraulic Engineering. 115: 101. doi:10.1061/(ASCE)0733-9429(1989)115:1(101)

[27] [27,2] [27,3] [27,4] [27,5] [27,6] [27,7] Annuals of Disas. Prev. Res. Inst., Kyoto Univ., No. 58 B, 2015 - Abrasion Damage Estimation of Sediment Bypass Tunnels: Validation and Comparison of two Prediction Models - Christian AUER, Robert M. BOES (Laboratory of Hydraulics, Hydrology and Glaciology, ETH Zurich, Switzerland) and Tetsuya SUMI

[28] 12th International Conference on Hydroscience & Engineering - Hydro-Science & Engineering for Environmental Resilience - November 6-10, 2016, Tainan, Taiwan - Abrasion Damage in Sediment Bypass Tunnels - Christian Auel, Tetsuya Sumi - Water Resources Research Center, Disaster Prevention Research Institute, Kyoto University - Kyoto, Japan – page 3, equation 6

[29] <https://www.focus-economics.com/commodities/base-metals/steel-europe/> - FOCUSECONOMICS, Gran Via 657, E-08010 Barcelona, Spain - info@focus-economics.com

[30] [30,2]

<https://www.xe.com/currencyconverter/convert/?Amount=1&From=EUR&To=USD>

[31] Shields, A. (1936). Anwendung der Aehnlichkeitsmechanik und der Turbulenzforschung auf die Geschiebebewegung [Application of similarity mechanics and turbulence research on shear flow]. Mitteilungen der Preußischen Versuchsanstalt für Wasserbau (in German). Vol. 26. Berlin: Preußische Versuchsanstalt für Wasserbau.

[32] Sediment bypass tunnels to mitigate reservoir sedimentation and restore sediment continuity – R.M. Boes, C. Auel, M. Hagmann & I. Albayrak - Laboratory of Hydraulics, Hydrology and Glaciology (VAW), ETH Zurich, Switzerland - DOI: 10.1201/b17397-27 – September 2014 - Reservoir Sedimentation – Schleiss et al. (Eds) - © 2014 Taylor & Francis Group, London, ISBN 978-1-138-02675-9